University of Stavanger

Faculty of Science and Technology

MASTER'S THESIS

Study program/Specialization: Petroleum Geosciences Engineering	Spring, 2013 Open
Writer: Sveinung Hatløy	(Writer's signature)
Faculty supervisor: Udo Zimmerman Co-supervisor(s): Ingunn C. Oddsen	
Title of thesis: **From Cold to Hot: Post- Hirnantian Sedimentary Basins in Bolivia- A Source Rock for Hydrocarbon Deposits in The Andes? – A Case Study of the Uncía and Catavi Formations.**	
Credits (ECTS): 30	
Keywords: Bolivia, Uncía Formation, Catavi Formation, Petrography, Heavy minerals, Petroleum geology, Provenance, Reservoir Characterization	Pages: +enclosure: Stavanger, ……

From Cold To Hot: Post- Hirnantian Sedimentary Basins in Bolivia- A Source Rock for Hydrocarbon Deposits in The Andes? – A Case Study of the Uncía and Catavi Formations.

By

Sveinung Hatløy, BSc

MSc Thesis

Presented to the Faculty of Science and Technology

The University of Stavanger

The University of Stavanger

June 2013

Acknowledgements

First and foremost, I would like to start by showing my appreciation and gratitude towards my supervisor Dr. Udo Zimmerman providing me with the possibility to conduct and complete this thesis. Also, for being a great teacher and mentor throughout these last 5 years at the University of Stavanger.

Furthermore I would like to thank Ingunn C. Oddsen for help and guidance with the Scanning electron microscope, your help is greatly appreciated. A special thanks goes to my friend and fellow student Trine Mehus, who has been full of encouragement and good advice since the sampling in Bolivia .

Last but not least those of you at home, for supporting me throughout the entire length of this process, I am forever grateful.

Abstract

From Cold To Hot: Post- Hirnantian Sedimentary Basins in Bolivia- A Source Rock for Hydrocarbon Deposits in The Andes? – A Case Study of the Uncía and Catavi Formations.

Sveinung Hatløy, BSc Petroleum Geology

The University of Stavanger, 2013

Supervisor: Udo Zimmerman

Co- Supervisor: Ingunn C. Oddsen

Two formations, Catavi and Uncía, comprise sedimentary rocks from Llandovery to possibly latest Pridoli rocks deposited in the Eastern Cordillera, northeast of La Paz. The main lithologies for the Uncía Formation are marine pelitic sediments with gradually more frequent arenaceous interbedding toward its top, where it meets the conformable Catavi Formation. Deposited during the Pridoli the Catavi Formation consists of interbedding of sand and shale deposited in a shallow shelf environment. Catavi and Uncía Formation lies in direct stratigraphic relationship to the diamictite bearing Cancañiri Formation consisting of post-glacial black shales deposited during Late Ordocivian along the Gondwana margin. Therefor a study focusing on composition using quantitative and petrological tools is ideal to determine their provenance, source and paleohistory. The provenance of the Uncía Formation points to a source or sources very close to the depositional areas as sorting effects did not play a role: shales and sands have the same trace element signature. Abundant pyrite,

even rounded grains in the heavy mineral fraction let assume an environment with low abundance of oxygen. However, organic matter is not anymore or has never been preserved. As the sandstones of this formation contain a variety of arc-related geochemical proxies one source might have been a Mid Ordovician succession, not anymore exposed or covered, in proximity, and the underlying pyrite-rich Cancaniri Formation (Mehus, 2013). The depositional environment changes towards the younger rocks (the Catavi Formation), with less preserved pyrite and even less organic carbon. The sources for this formation might have been more variable but point to longer transportation of the grains.

The lack of any characteristics for larger organic matter, with even absence of common graptolites in the shales, point to a deposition under partly anoxic conditions but without abundant organic matter. Hence, it seems that the post-Hirnantian faunas did not recover until the Uncía Formation in contradiction to northern Gondwana successions, today deposited in Europe where Silurian rocks are rich in organic matter. This implies for Bolivia that hydrocarbon reservoirs have been sourced from other rocks.

Table of Contents

1.0 INTRODUCTION

1.1 Post-Hirnantian glaciation

The end Ordovician is marked by two phases of mass extinction that coincided with major sea-level changes associated with the development and retreat of Gondwanan glaciation (Benchly, 1988). Early post-glacial, transgressive sediments, supposed to be organic-rich black shales were a frequent feature of the northern Gondwana continental shelf during the late Ordovician to early Silurian (Howard et al., 2005), documented in Arabia, central and south Europe, Africa and South America. The record of the Ordovician-Silurian transition within the western (South American) margin of Gondwana is characterized by a diamictite-bearing unit which overlies several different Ordovician units, and underlies mid Silurian shales, more specifically in the Peru-Bolivian basin (Martinez et al. 2011).

These rocks, which can contain up to 10% total organic carbon, combine one of the world's major hydrocarbon source rocks. The origin of these black shales is uncertain, by the fact that modern open shelf settings are only subject to seasonal anoxia (Tyson, 1996; Tyson and Pearson, 1991) and black shales are not currently forming naturally on modern shelves. However, Mehus (2013) could show that the black shales in the Cancañiri Formation do not contain siginificant organic matter (less than 1 % in most of the rocks).

The Uncía and Catavi Formations lie in direct stratigraphic relationship to the diamictite bearing Cancañiri Formation consisting of post-glacial black shales deposited during Late Ordocivian along the Gondwana margin. Therefor a study focusing on composition using quantitative tools is ideal to determine their provenance, source and paleohistory.

1.2 Objective of the study

The study here described focuses on post-Hirnantian clastic sedimentary rocks from Silurian age, outcropping northeast of La Paz, Bolivia, in the area of La Cumbre, (Figure 1). Two formations (Uncía and Catavi) where sampled to compare similar data in terms of reservoir characterization and basic geological information using whole rock geochemistry, SEM-EDS-BSE-CL and basic petrography to reveal the signatures and in terms the geological history. This in addition to measuring organic carbon will enable us evaluate the petroleum significance and of the post- Hirnantian sediments in Bolivia.

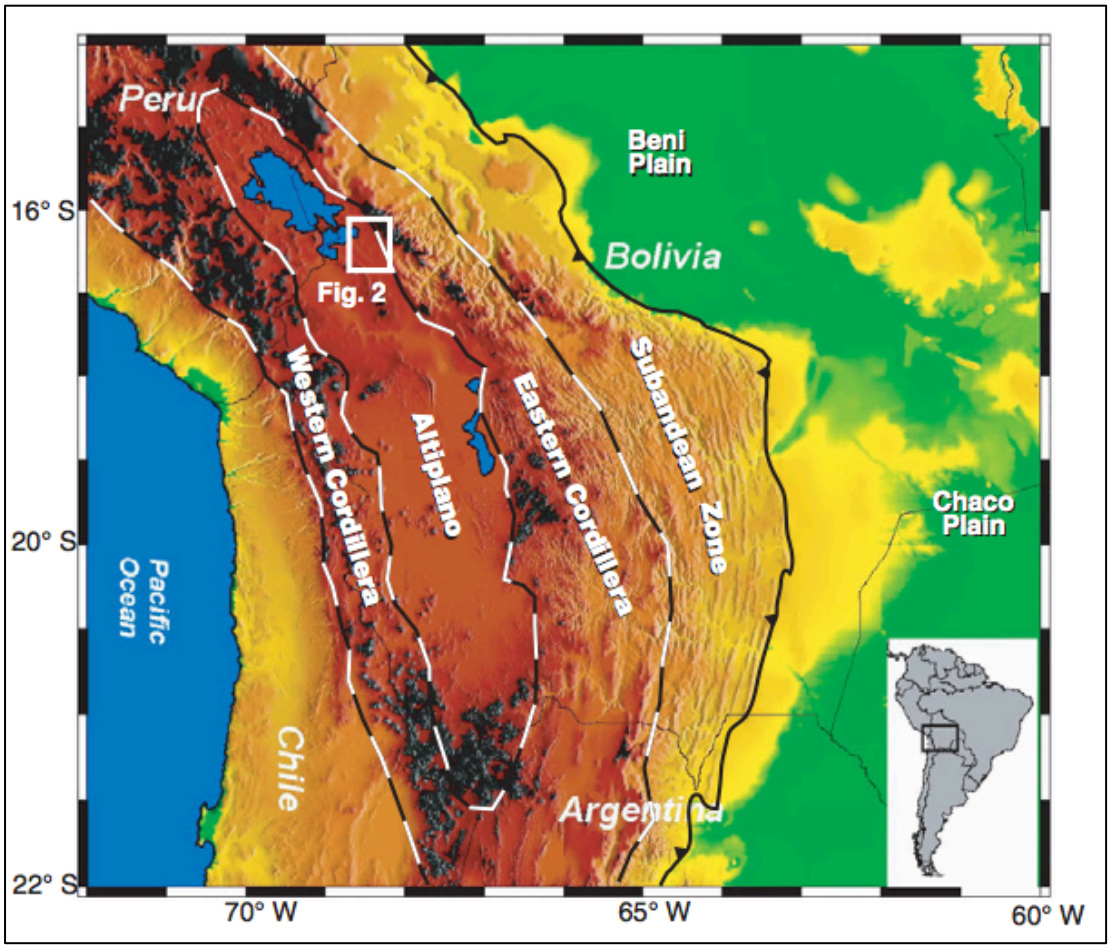

Figure 1 – Map showing regional topography of the central Andes (after Murray et al. 2010). Major physiographic divisions are separated by dashed lines (after Isacks, 1988; McQuarrie et al., 2005). Darker colors (orange, red, gray, black) define regions of higher topography (>3.5 km). Box shows location of Figure 2.

1.3 Outline of the study

In the presented study the sampled area will firstly be introduced, followed by the regional geology and stratigraphy related to the studied area. Then, a presentation of the methodology relevant for this study will follow, before the collected results and analysis are described and later discussed. Lastly, the data will be merged in a geological interpretation and petroleum evaluation of the area, where the key question will be to investigate Bolivias response to deglaciation and if this will be visible in terms of organic rich rocks.

1.4 Working title and analytical techniques

"From Cold to Hot: Post- Hirnantian Sedimentary Basins in Bolivia- A source rock for Hydrocarbon Deposits in The Andes? – A Case Study of the Uncía and Catavi Formations."

The rocks were sampled in Bolivia, preparations were done in Stavanger, Canada, Argentina and Australia. Heavy mineral separation was executed in Australia by the company GeoTrack and mounted in Stavanger. The Scanning Electron Microscope (SEM) is located in Stavanger, at the University of Stavanger. Also Backscattered Electron (BSE) images, Energy Dispersive spectrometer (EDS) and Cathodoluminescense (CL) is done, supported by geochemical (GC), petrographical and organic carbon analysis.

1.5 Regional geological setting

This study is located in Bolivia, c. 4 km Southeast of the city La Paz on the road towards La Cumbre, in the Eastern Cordillera (EC). Two formations were sampled featuring clastic sedimentary rocks of Silurian age formally named the Uncía (Vargas, 1970; Suaréz Soruco, 2010) and Catavi Formations (Koeberling, 1919).

Bolivia lies in the heart of South America, landlocked, bordering Chile, Peru, Brazil, Argentina and Uruguay. The country is built up of five major physiographic provinces, closely coinciding with structural units (Kley et al. 1997), (Figure 1). To the west we find the Western Cordillera (WC) generated as a result of the subducting Nazca plate beneath the South American plate, creating a 700 km stretch along the west coast of South America comprised of active and dead volcanoes with elevations up to 6500 meter above sea level. Moving eastward the intermontane high plateau of the Altiplano borders the range of the Eastern Cordillera, which forms the backbone of the Bolivian Andes. Further east you find the lower positioned Interandean zone and the Sub-Andean Ranges.

The Altiplano and EC, together, form the "Central Andean Plateau" (Gubbels et al., 1993), which is underlain by a continental crust with a thickness of at least 70 km (Wigger et al., 1994; Zandt et al., 1994). The Altiplano is an internally drained foreland basin with an average altitude of about 3800 m, composed of a thick Tertiary and Quaternary cover with additional volcanic rocks (Kley, 1997), (Figure 2). Which, in the south part of Bolivia on its eastern margin is overthrusted by the EC on the west verging San Vincent thrust system (Hérail et al., 2000) The EC is mainly composed of epimetamorphic (low grade metamorphic) marine sediments of Ordovician age that are in localities unconformably overlain by Cretaceous and/or Tertiary sediments and volcanic rocks.

The geological evolution of Bolivia and the central Andean system during the past 500 My was largely controlled by the geodynamics of the South American margin of western Gondwana. The Late Cambrian-Early Ordovician margin was initially a passive margin, which became an active margin during the Middle Ordovician compressional episode and further controlled by a large-scale transtensional or transpressional event from Late Ordovician to the Triassic. During most of Late Ordovician until the Paleogene, Bolivia was located close to the southern tip of a trough running parallel to the Pacific margin of South America that generally deepened toward the north or northwest along its axis. This trough, referred to as the Bolivian-Peru basin by Sempere (1995) was restricted towards the south by the Sierras Pampeanas area located in northwestern Argentina. As a result of this geometry, from Late Ordovician to early Paleocene, marine transgressions flooded into Bolivia from the northwest. Between Late Ordovician to the Late Jurassic, most of Bolivia acted as a large sedimentary basin only subjected to local compressional deformation. Mainly depositing marine strata until Early Triassic, after which continental deposition dominated, however with six restricted marine transgressions, last recorded in Late Miocene.

Since the Late Ordovician to the Mississippian the facies evolution was characterized by a high rate of subsidence of the marine foreland, which was filled with thick, shallowing upward sequences with northeastward onlaps. Fluctuating sea level processes and glaciomarine successions are recorded in this period, overlain by shallow marine carbonates, marls, sandstones, evaporites and some eolinites deposited during the Pennsylvanian to Early Triassic time. The stratigraphy deposited during Silurian-Devonian/Middle Jurassic closely resembles that of the widespread Chaco-Paraná basin in Brazil, eastern Paraguay, northwestern Uruguay, and northeastern Argentina (Sempere, 1990). Implying that relatively stable and cratonic conditions were present (Oller and Sempere, 1990). Todays Sub-Andean Beni-Chaco basin, into which Andean deformation still is propagating is the undeformed

remnants of the Bolivian-Peru basin. After the Middle Triassic rifting was aborted and the Bolivian basin behaved in a cratonic way until it was merged into the Andean system due to the start of transtension along the margin in the Late Jurassic, further becoming part of the Andean foreland domain in early Senonian time. The extensional process resulting in the opening of the Atlantic Ocean from Latest Jurassic on, when South America broke up and the old depocenter have been reduced by compressional movements and large strike-slip systems, where the western part of South America was involved on the Pacific margin geotectonic system (Sempere, 1994).

Andean thrust deformation propagated into Bolivia during the Oligocene until today, making the Bolivian Andes comparatively young (Sempere et al., 1990), created by advancement through a series of décollement levels in Paleozoic shales in the Bolivia-Peru basin. The Paleozoic basin and its sedimentary infill has acted as a control on the geometry of the Andean deformation (Sempere et al., 1989, 1991; Hérail et al., 1990), suggesting Phanerozoic topography was considerable in the Bolivian orocline, involving high shortening in its northwest trending segment and trans-current motion.

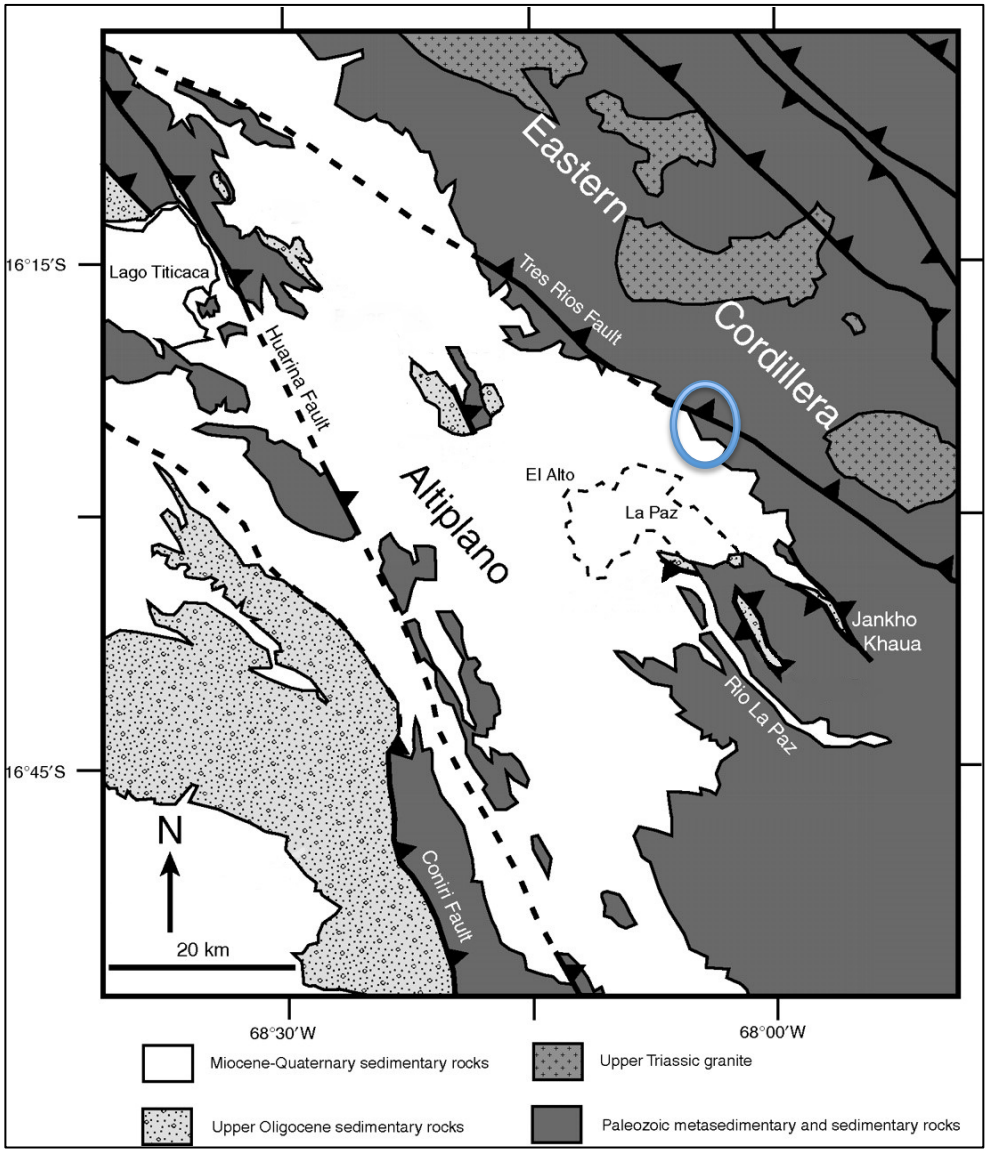

Figure 2 - Regional geologic map of the La Paz (Bolivia) region along the Eastern Cordillera– Altiplano boundary showing the generalized geologic units and major faults, blue circle denotes sampling area, (modified after Murray et al. 2010).

1.6 Stratigraphy

The stratigraphy of the Cordilleran Cycle sediments in the Bolivian Eastern Cordillera are widely distributed in the Huariana Fold Belt and in the Andean – Subandean Belt, deposited as infill of a wide intracratonic basin, with sediments coming from west and south. The Late Ordovician to Silurian stratigraphic sequence in the Altiplano and Eastern Cordillera is built up by the Cancañiri, Llallagua, Uncía and Catavi Formations, (Figure 3). The shallow shelf

marine pelitic sediments of the Uncía Formation lies above the diamictie bearing Cancañiri Formation and the turbiditic Llalluga Formation, which is thinning westward, creating a direct contact between the Cancañiri and the Uncía Formation. The Uncía Formation indicates a Ludlovian age determined by *Saetograptus-Phragmolites-Dualina* and *Harringtonina* zones (Surárez-Riglos et al., 1994). Gradually towards the top, arenaceous interbedding is more frequent where it is in contact to the conformable overlying Catavi Formation. Starting with a sandbank generally carrying the *Clarkeia antisiensis* brachiopod, the Catavi Formation was deposited during the upper Silurian (Pridoli), in a shallow shelf environment with coastal influence. In known localities, the Catavi Formation ends with a pelitic horizon named the 'Ventilla' by Koeberling (1919), which is attributed to the base of the Devonian, however this horizon is more frequent absent and therefor the formation grades transitionally into the Vila Vila Formation (Fricke et al., 1964).

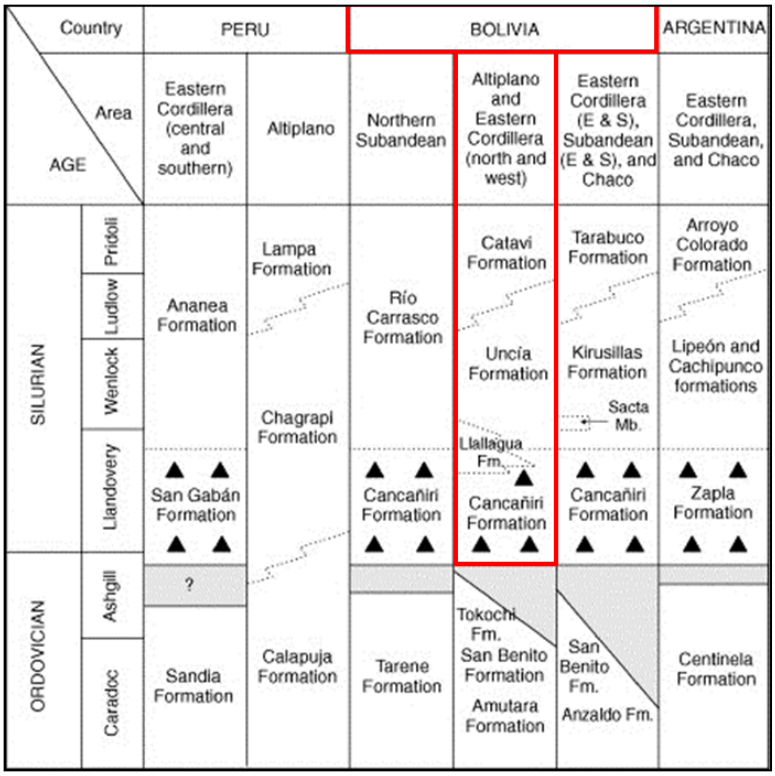

Figure 3 – Stratigraphy of Ordovician – Silurian rocks in Central Andean, with emphasis on the Altiplano and Eastern Cordillera. (Martinez and Grahn, 2007).

1.7 Sampling

The material studied for this thesis comprises of clastic sedimentary rocks from the Uncía and Catavi formations collected along the Ruta Nacional 3 near the locality of La Cumbre, North East of La Paz (Bolivia): (i) Uncía formation was sampled at an exposure 1,5 km Southwest of Lake Represa Incachace (S16° 25' 03.0'', W68° 03' 18.4''), the second formation, (ii) Catavi was sampled 1.8 km apart from stop (i), towards La Paz (S16° 25' 47.7'', W68° 03' 57.7''). Several samples (approximately 20) were taken from each formation along exposed road cuts from coarse sandstone to silt and shales (Appendix A, Fig A1 and A2). Some of the samples were collected for detrital zircon dating, heavy mineral analyses and cathodoluminescence (CL), other for geochemistry (GC), X-Ray Diffraction (XRD) analysis and petrography. Besides detrital zircon dating and XRD, results of the other methods are presented here.

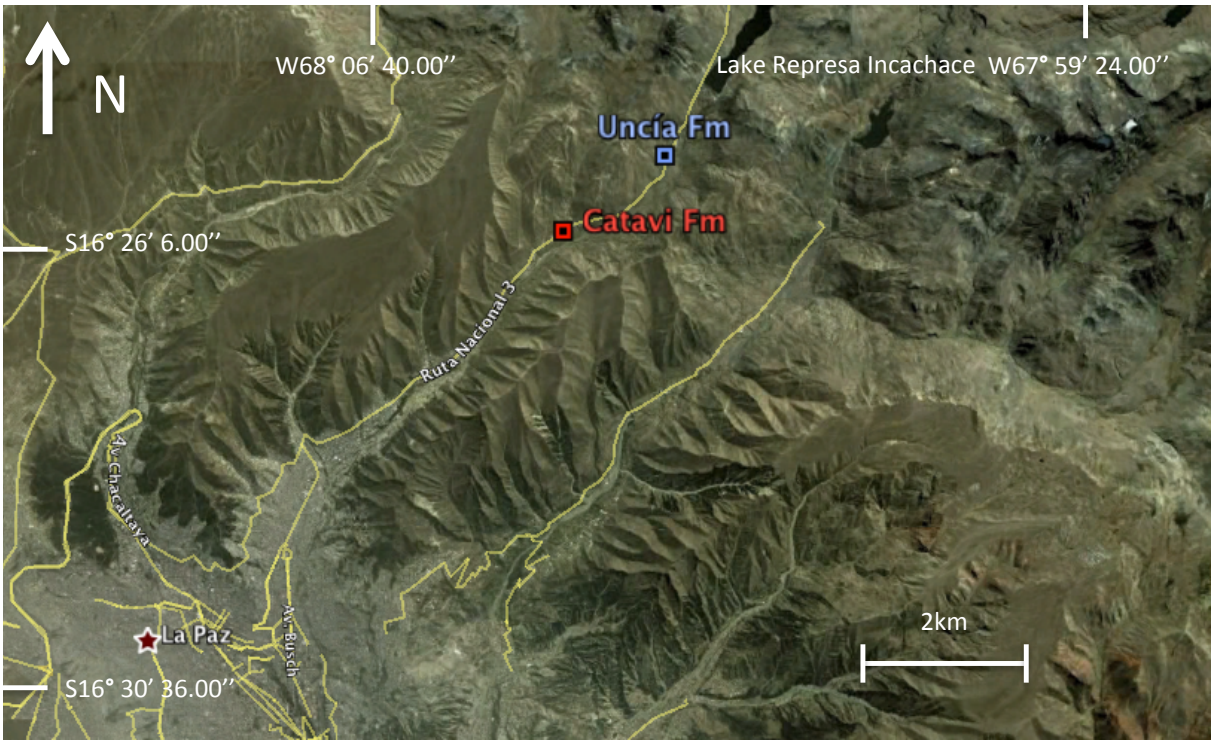

Figure 4 – Location of sampled formations, northeast of La Paz. (Modified after image from Google Earth.)

2.0 PROCESSING AND ANALYTICAL METHODS

2.1 Petrography

The making of thin sections for petrographic investigation started with cutting flat edges along the surface of interest on the rock samples. The one edge on each specimen was then polished with silica carbon powder #220, #320, #600 and #1000 until it was perfectly flat. Next step was to mount the rocks on rectangular glass plates using epoxy glue, SpeciFix-20. We polished the glass plates before mounting so the glue could stick better, also important here to measure the thickness of the glass plate for further cutting. The glue consists of a resin and a curing agent, mixed in 7:1 ml ratio, stirred slowly for 3 minutes to avoid air bubbles, and put to rest for 3 minutes before it is applied. The application process is done by adding two drops of glue on the glass and place the rock with the smooth surface on top. By adding pressure, air bubbles are squeezed out. The samples are set to cure for 24 hours.

After this process the rock is cut in a thin section, by a Struers Actom-50 cutting machine, and further polished with silica carbon powder until the rock section is 25 microns thick. Thin section from Catavi Formation was not executed do to malfunction in equipment, therefor petrography is only conducted for Uncía Formation sandstone.

2.2 Milling

2.2.1 AUTOMATED MILLING FOR GEOCHEMISTRY

For geochemical analysis the selected rocks were milled in an automated agate mill. This procedure milled the rock grains to an extreme fine mesh, done in a Retsch RS200 milling machine. Each sample was milled at 700 rpm, the speed is limited by the properties of the agate beaker. Each shale sample was more or less done in 2-3 minutes in the machine, while

the sandstones were more difficult to mill. The sandstone samples easily jammed the beaker rings and we had to hammer the rock samples into smaller pieces. Sandstone samples needed about 5-10 minutes in the milling machine until being finely powdered. From each sample we milled at least 10 grams, the samples were weighed and packed. The agate beaker was cleaned with water and acetone after each sample, and with pure silica sand when switching between formations. A hair dryer was used to dry the beaker and get the humidity out of the form.

2.3 Heavy mineral preparation

2.3.1 Heavy Minerals separation techniques after Mange and Maurer

Heavy minerals have been separated according to common well known processes with heavy fluids, then glued, polished and fixed on small epoxy disks. The procedure of isolating heavy minerals from solid rock such as sandstone and shale start with decreasing the rocks size. It needs to be reduced to 5 mm chips, done with a mechanical instrument such as a roller-crusher or a jaw-crusher. A mortar and pestle can also be sufficient, applying vertical exerted force avoiding damage to the original size and shape of the grains. Further acid digestion is necessary to remove carbonates, alternatively H_2O to remove salts. Commonly HCl (10%) or CH_3COOH (10%) is used, note that HCl can damage phosphates, which can ruin apatite in fission tracks, ruining the possibility to do studies of thermal history in a formation. With using only CH_3COOH (acetic acid) no damage will be done to the phosphates, but this is a longer process, taking 1-3 days. (Also some heating would be necessary.) With silica-cemented rocks disaggregation is best achieved using KOH or NaOH solutions. Though this can do severe damage to siliciclastics.

The sieving process is required to get the appropriate grain sizes. A necessary step for removing finer particles from loose sands and disaggregated materials. This is done by a technique called wet sieving, were the material is sprayed with water in a sieve with 0.063 mm or 0.053 mm aperture. The sieve is then placed in a mechanical shaker for 10 min, and dried afterward. The material can be washed to reduce the amount of clay minerals.

Separating the heavier fractions is commenced using high-density liquids. The idea is to allow the minerals with a specific density below 2.9 g/cm^3 to float while the heavier particles submerge, the technique is called gravity settling or funnel separation. Liquids normally used for separation:

Liquids	Density at 20 °C
Bromoform (tribromoethane)	2.89 g/cm3
Tetrabromoethane (acetylene tetrabromide)	2.96 g/cm3
Methylene iodide (di- iodomethane)	3.32 g/cm3
Clerici´s solution	4.24 g/cm3

Table 1 - Heavy liquids (from Mange and Maurer, 1992)

The liquids above do produce toxic fumes and have to be applied in a fume cupboard. Protective goggles and gloves are also necessary precautions. Further a dry and weighed sample (max. 10 g) is added to the liquid, stirred to get all grains wet. The process normally takes 6-8 hours to get all the heavy particles accumulated at the bottom. Then a pinch clip is opened slowly allowing them to flow out into a filter paper in the lower funnel. The pinch clip is then closed so the rest of the particles are stored in a separate container.

The sampled heavy minerals are rinsed with alcohol or acetone and set to dry. The funnel is washed with a heavy liquid to clear out any grains, and then the process continues to everything is separated. The heavy fractions, when dry, go through a Franz magnetic separator. This is a machine separate the loose fractions according to their magnetic character. The respective fractions and their specific separating densities and angles:

- Magnetic fraction (at 10° full scale in Frantz magnetic separator, and $\delta > 2.8$ g/cm^3).
- Apatite fraction (non magnetic grains with δ from 2.8 to 3.3g/cm^3).
- Zircon fraction ($\delta > 3.3$ g/cm^3 with slight magnetism at 2° in Frantz magnetic separator).

The heavy mineral grains should now be glued into an epoxy disk. 2 samples from each fraction were mounted into rings to receive a total of 12 samples. A double-sided tape was glued on two square glass plates, onto the tape we placed the rings with a diameter of 1,5 cm and a height of 1,2 cm. The grains were dispersed on the tape inside of the rings. Then Epofix glue was poured on top of them, until the epoxy rings were 2/3 full. The glue consists of two separate liquids, Speci Fix Resin and Speci Fix-20 Curing Agent, which are mixed 3:25, and stirred slowly for 3 min to a homogenous liquid. To get a representative selection of the grains independent on density and size, we spread the entire sample on a clean sheet of paper. A razor blade was used to separate an amount of grains used for the specific fraction. The Epofix glue needed 24 hours to solidify. The disks were then polished in #600 and #1000 silicon carbide powder manually. The rings were polished until the grains were visible on the top of the glue. The mounts were further processed in a Struers Tegra polishing machine, in two steps using 3 and 1μm diamond powder disks for about 4-5 min on each step. Afterwards, pictures were taken with a light microscope to be used as maps when using the scanning electron microscope.

Selected samples from the two exposures were sent for heavy mineral separation. This

resulted in two sample sets, one from the Uncìa Formation and one from the Catavi Formation. The heavy mineral separate were divided in a (i) zircon-fraction with unmagnetic heavy minerals having a specific density above 3.32 g/cm^3; (ii) apatite-fraction (unmagnetic; > 2.89 g/cm^3) and (iii) magnetic fraction (>2.89 g/cm^3).

2.3.2 COATING OF MOUNTED HEAVY MINERAL FRACTIONS

The last step before the electron microscope analyses was to coat the samples. Coating is a technique used to cover a surface with a conductive material, in this case carbon (C), inhibiting accumulation of static electricity on the sample during electron irradiation, reducing thermal damage and improving secondary electron emission. The coating also increases the ability for electrons to emit from the specimens increasing image quality. Firstly the samples were cleaned in a sonic bath, rinsed with ethanol removing organic residue and a high-pressure air gun to remove any dust particles. The samples were further placed in a Leica EM SCD500 high vacuum sputter coater with a surrounding airtight glass container. A lid is placed on top containing a C-thread and the machine creates a vacuum around the sample. When a vacuum is achieved the C thread releases a glow discharge evaporating the material. The vacuum allows the vaporized C particles to travel onto the polished sample were it condense back to a solid state. When completed, after c. 5 minutes, the mounts are covered in a 20 nm thick film of C ready for SEM analyzes. Next a conductive Carbon tape was placed on the sample allowing electron flow through the sample and the sample holder. The coated samples were mounted onto aluminum stubs before SEM analysis. The C coating and C tape gave of readings on the EDS, (Appendix E).

2.4 Analytical methods

2.4.1 PETROGRAPHY

Petrography analyses were conducted using a Zeiss AXIO light microscope with an AxioCam ERc 5s camera connected to a computer.

2.4.2 SEM-EDS-BSE-CL

The samples were analyzed with a Zeiss Supra 35 VP featuring a Scanning electron microscope (SEM) with a Back scattered electron (BSE) detector and Cathodoluminecense (CL) at 20 kV. Energy dispersive spectrometer (EDS) is also included with an EDAX detecting unit, combined with EDAX Genesis software for chemical identification.

2.4.3 GEOCHEMISTRY

Inductive Coupled Plasma – Mass Spectrometry (ICP-MS) analyses were performed by ACTLABS (Ontario, Canada) for geochemistry. Sample powders were dissolved in lithium metaborate flux and the resultant bead rapidly digested in dilute nitric acid. Further specifications can be downloaded at www.acmelab.com.

3.0 RESULTS

The results include siliciclastic rocks from two formations, Uncía and Catavi. The stratigraphic relation is defined as post- Hirnantian with a Llandovery base (Surárez-Riglos et al., 1994), overlying the late Ordovician post- glacial Cancañiri Formation and the westward thinning Early Silurian Llalluga Formation, with an upper Pridoli boundary defined by the overlying early Devonian Vila Vila Formation (Fricke et al., 1964).

3.1 Petrography and mineralogy

The sandstone of the Uncìa Formation is characterized by mainly quartz, muscovite, hematite, small amounts of feldspar and zircons. The quartz is well sorted consisting of white and grey angular grains, (Figure 5). Hematite is observed in larger compartments/veins, suggestive for intrusion and deposition by a secondary iron rich fluid. Muscovite is found as purple and green elongated grain, surrounded by clay materials primarily consisting of kaolinite and chlorite. The section contains of 5-10% matrix due to closely spaced grains. The source is believed be close, and possibly an eroded fine-grained sandstone as most of the grains are angular.

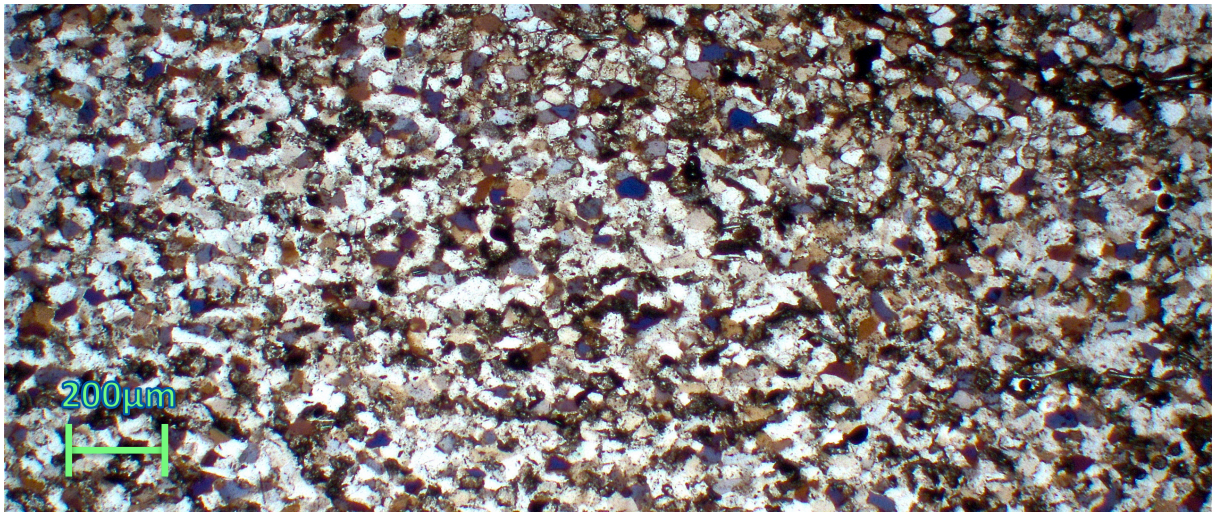

Figure 5 –Thin section showing abundance of quartz, with a hematite vein in the upper right corner.

3.2 Heavy mineral fractions (HM)

Heavy mineral fractions were extracted from Uncía and Catavi Formation and studied using SEM, EDS, BSE and CL. Three separate samples were used from each formation, named in the order which they will be described; apatite-, zircon-, and magnetic fraction. The fractions are stratigraphically divided into Catavi - CAT and Uncía - UN, Table 2. Two sample sets from each fraction were made for each separate formation, however, in the observations these results will be combined.

Formation	Apatite	Zircon	Magnetic
Catavi (CAT)	CAT-A1/CAT-A2	CAT-Z1/CAT-Z2	CAT-M1/CAT-M2
Uncía (UN)	UN-A1/UN-A2	UN-Z1/UN-Z1	UN-M1/UN-M2

Table 2 – Heavy mineral fractions divided after formation and name.

3.2.1 CATAVI FORMATION

3.2.1.1 Apatite fraction

The dominant mineral for this fraction is apatite with 81% of the total sample, other heavy minerals in abundance are zircon 11% and rutile 5%. Heavy minerals detected in smaller quantities are monazite, ilmenite, muscovite, quartz and biotite was encountered as accessory minerals in combinations with heavy minerals, typically with rutile and zircon.

Apatite

The majority of the encountered apatite minerals have a size ranging from 40 – 100 μm, and have been subjected to mechanical weathering with sub-rounded to rounded features. Typically specimens have rounded edges or indentations, however they appear in solitude with no accessory minerals. Other apatite samples, on the contrary, are rectangular and

almost cubical with few signs of transportation. Their sizes are between 35 – 80 μm, and display accessory minerals such as feldspar and quartz and impurities of other heavy minerals such as monazite, (Figure 6).

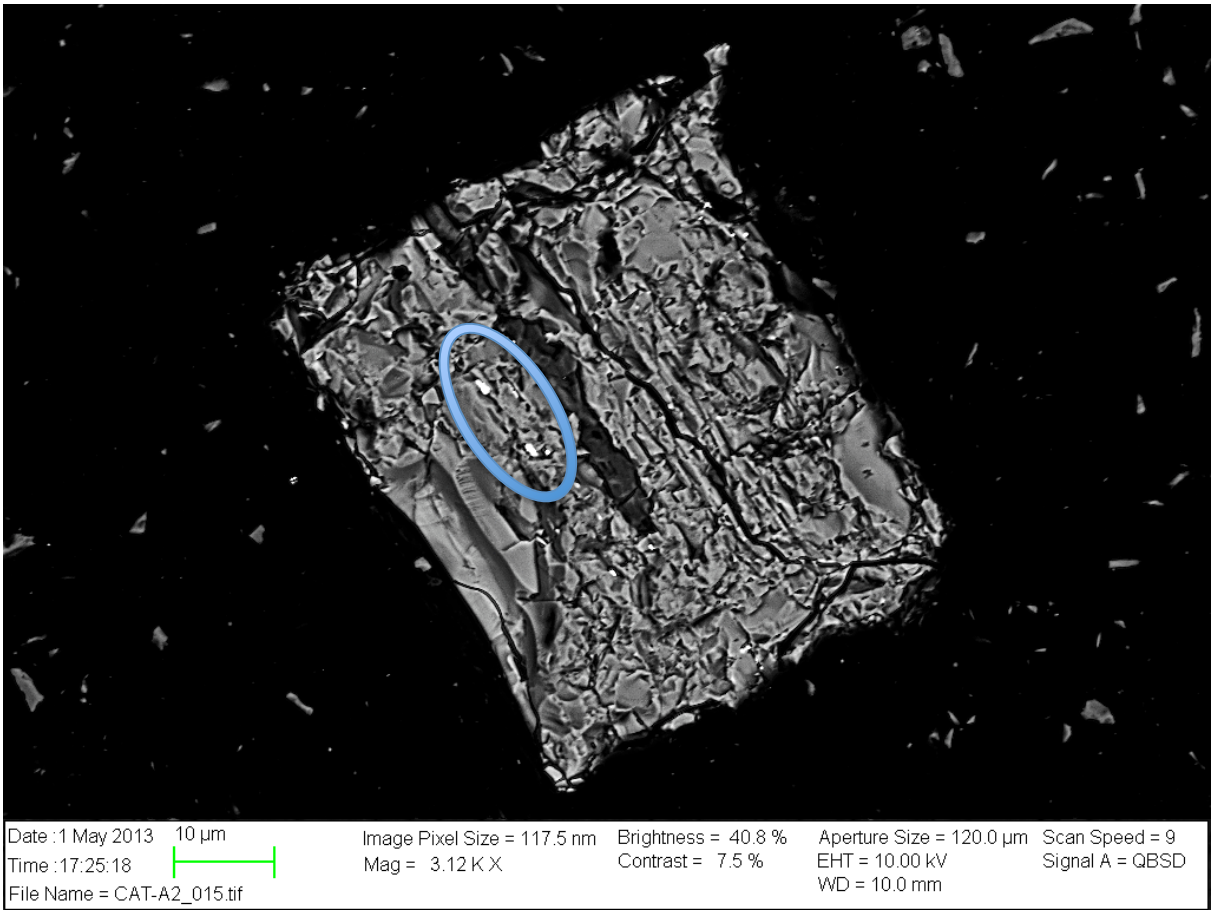

Figure 6 – Cubical apatite with monazite impurity, BSE micrograph.

Zircon

Zircons specimens range in size of 35 – 70 μm and show a combination of angular and rounded features. All samples are to some extent rounded, however some display a combination with angular edges. The zircons are all found alone.

Rutile

The discovered rutile specimens have a diverse physical appearance, a general size range is between 30 – 70 μm, and their form are typically rounded with some examples of angularity and indentation. Another specimen shows 3 to 7 μm long elongated rods, typical for authigenic rutile, found within a larger quartz grain, (Figure 7). Common for all samples is the coexistence with lighter minerals, primarily quartz and clay minerals.

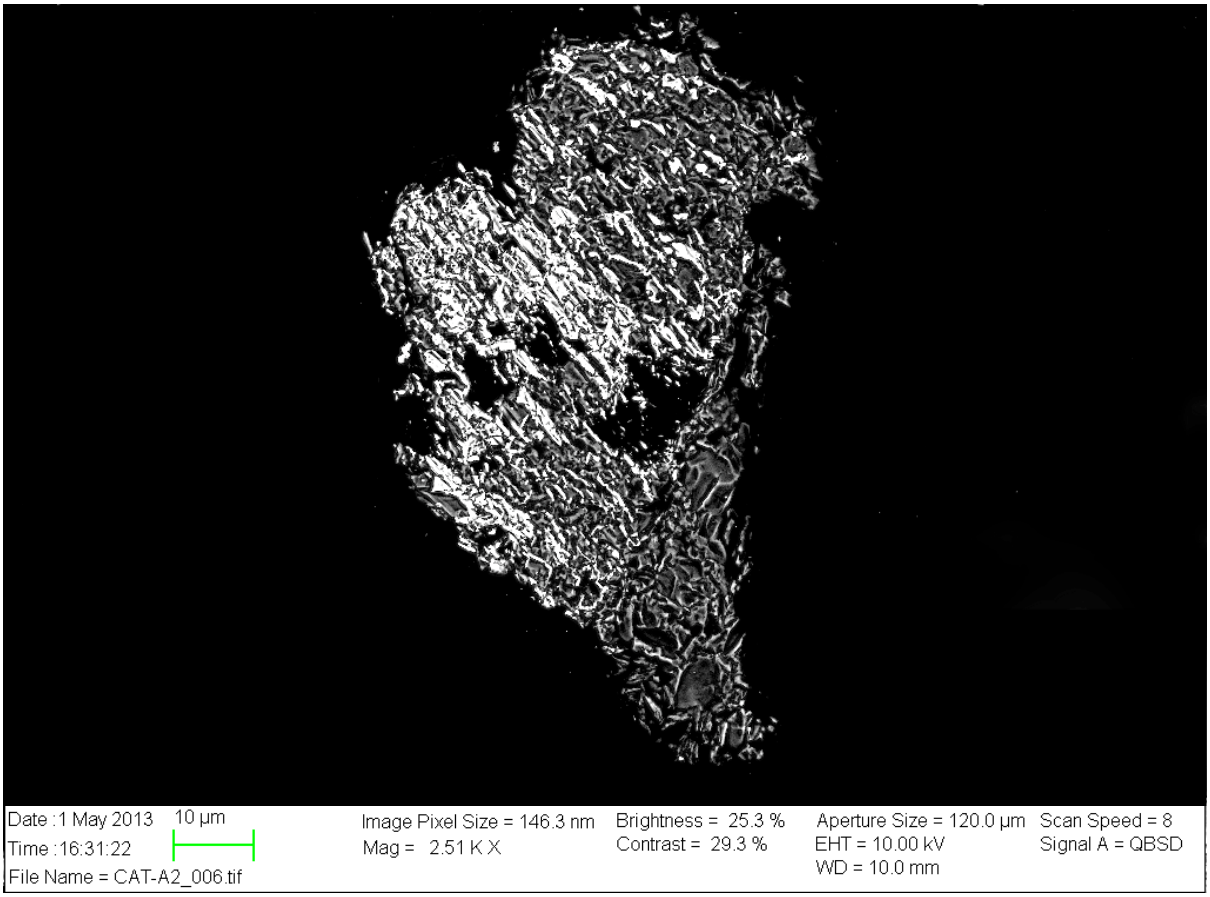

Figure 7 – Rutile represented as the bright white elongated mineral within darker quartz. BSE micrograph.

Other Minerals:

Monazite and ilmenite were detected as impurities on a micronscale in larger apatites and rutiles. Minor rounded albite has been found suggesting grinding during transport.

3.2.1.2 Zircon fraction

The majority of heavy minerals in the zircon fraction are zircons with a total of 55%, further more rutile has been abundant (43% of the measured grains). Other heavy minerals found were apatite and titanite. Muscovite, albite and quartz accompany many of the heavy minerals often as a host with fractionated heavy minerals, but also in cases as fragments in the heavier minerals.

Zircon

Great amounts of the total heavy mineral count in this specimen show zircon minerals. Their shapes show signs of physical weathering noticed by a majority of rounded and fractionated samples, however angular samples was also in encountered, (Figure 8). The weathered specimens range from 40 – 80 μm. There are further some samples that have cubic features containing larger specimens ranging in-between 25 x 95 μm. There was not discovered any impurities or accessory mineral in combination with the zircons.

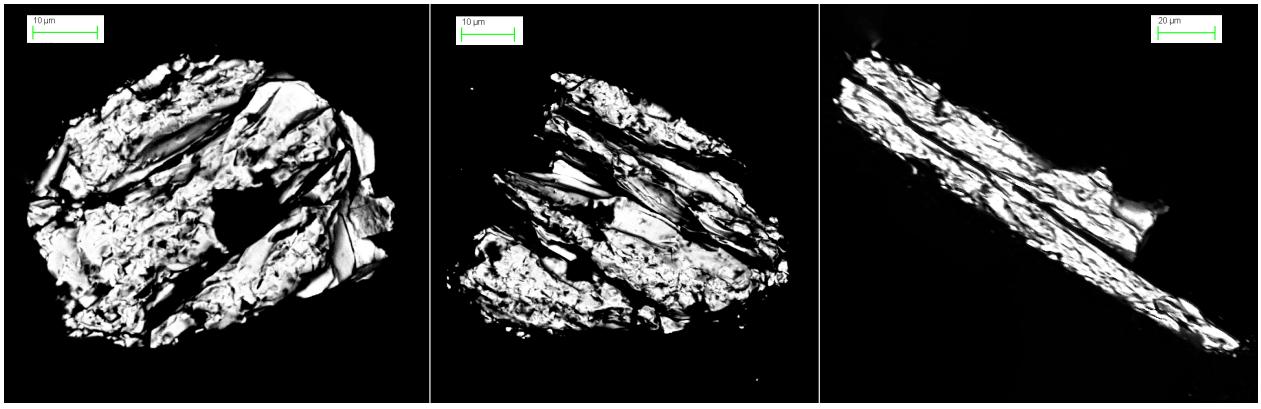

Figure 8 – Samples of zircons with various physical features in the Catavi Formation. BSE micrograph.

Rutile

Rutiles exhibit specimens in various forms, sizes and in combination with different minerals. Three different groups are observed; sub-rounded, angular and fragments. The rounded

specimens are 50 – 120 μm in diameter, however some angularity is present in the larger samples. These samples coexist with muscovite, biotite and quartz. The angular rutiles are both elongated and cubic, ranging in with and length 40 x 80 μm, and are often found with no accessory mineral, however few samples are observed in association with quartz. The fragmented samples display a length of 40 – 80 μm, and could be sub-rounded specimens, who have endured extensive weathering due to exposure. They are found inside larger flakes of quartz, were the rim has crevasses and exposes quartz.

Other Minerals:

Apatite minerals were mostly rounded and < 35 μm, however specimens with angularity and fissures were discovered. Further, angular titanites were encountered together with rounded quartz minerals. There were also noticed small quantities of pyrite impurities in quartz associated with rutile.

3.2.1.3 Magnetic fraction

The sampled fraction shows different heavy minerals with a majority of ferrous heavy minerals. The samples displayed a majority of fayalite contributing 37% of the total composition, further major heavy minerals in abundance are monazite with 15%, magnetite 12%, zircon 8%, and rutile 6%. Smaller quantities of almadine have been discovered, however mainly as impurities and in association with other heavy minerals and lesser minerals such as quartz and micas.

Fayalite

Sampled fayalite show diverse sizes and shapes. Generally their sizes range between 60 to 120 μm, however smaller rounded fractions indicative of erosion display sizes < 60 μm. Fayalites that are angular typically have a larger size, however broken and weathered specimens show larger examples. Further, there are no encountered samples without accessory minerals, typically muscovite, biotite and quartz. Also impurities were documented but the chemistry could not be determined.

Monazite

Monazite specimens appear as single grains, impurities and in coexistence with other heavy minerals and lighter minerals. Therefor a great variety of size and shapes is observed. Single grains are < 65 μm with sub-rounded features. Elongated impurities are discovered in apatite specimens where sizes are < 1 μm. Also larger monazites with sizes between 10 to 15 μm coexisted within apatite and calcite grains, (Figure 9). Lastly, monazites were also observed together within muscovite, these specimens exhibit erosive features with size <30 μm in diameter with nearby impurities.

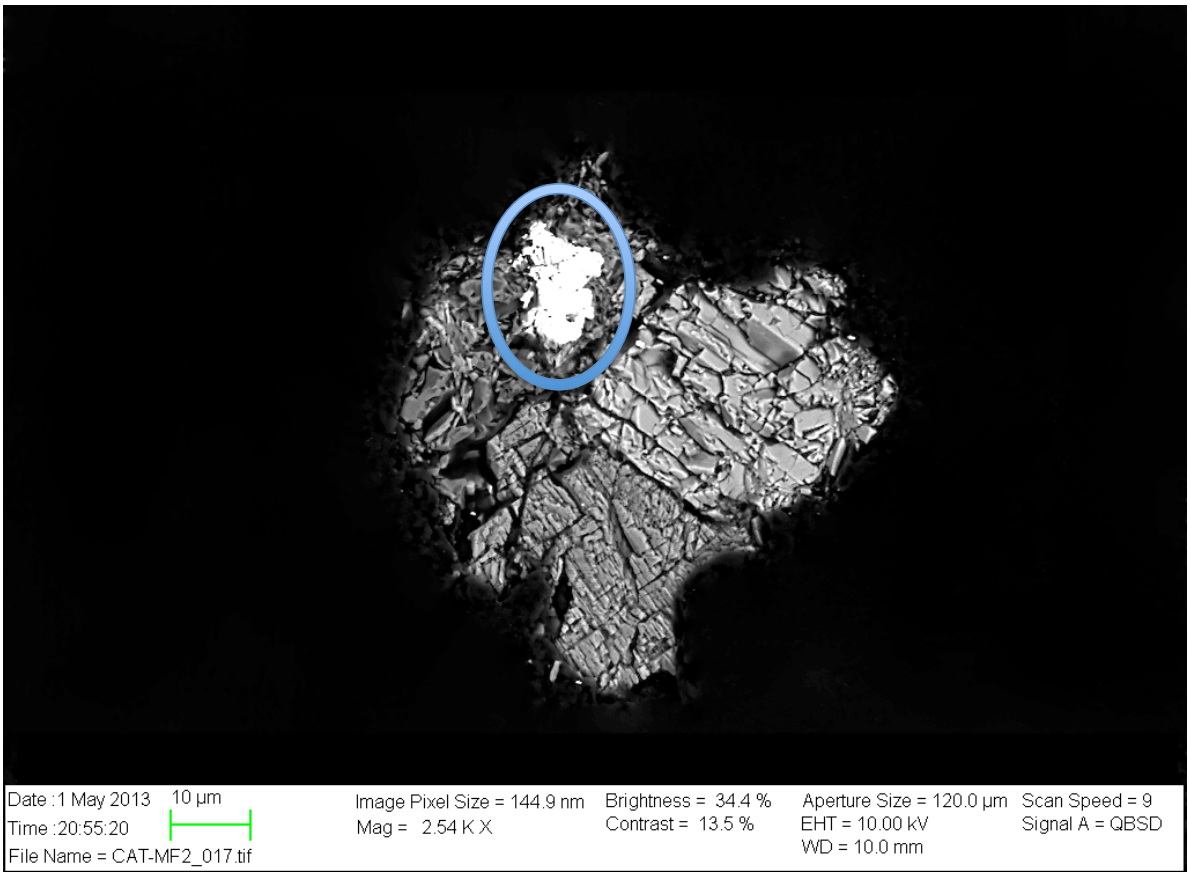

Figure 9 – Marked blue circle indicates monazite inside a calcite rich mineral, the lighter grey fragment to the right is composed of apatite. BSE micrograph.

Magnetite

Magnetite was generally observed as single grains sometimes with accessory mica particles. The features indicate erosion, due to rounded and fractures samples. Sizes range between 35 - 150 μm, where the fractured samples show the largest samples. A specimen contains a crystalline octahedral (Appendix E, Fig.E 1), which can indicate stable conditions for growth or a relatively close source.

Other minerals:

The entire fraction revealed a wide variety of heavy mineral. In addition to the previously mentioned minerals majorite and chromite were discovered as impurities in larger minerals. Zircon specimens were <30 μm in diameter, sub-rounded and generally encountered without

accessory minerals. The rutiles also showed evidence of erosion, with rounded samples inside larger flakes of quartz. Lastly, small numbers of apatite were encountered in association with calcite and mica, with monazite impurities.

3.2.2 UNCÍA FORMATION

3.2.2.1 Apatite fraction

The fraction is dominated by pyrite, encompassing 94% of the total content. Further, small amounts of rutile, zircon, bismite, nisnite and sillénite are discovered. There is great abundance of lesser minerals, most typically quartz and micas, in coexistence with heavier minerals.

Pyrite

Pyrite specimens revel angular, rounded and fragmented specimens. Most typical are the angular specimens which exhibit sizes from 30 – 150 μm, found in some cases associated with quartz, however the majority is encountered as single grains. Rounded grains are within the same size as the angular, typically in the lower end of the scale. They display elongated, almost elliptical shapes, with minor fragments of mica and quartz. Lastly the fragmented specimens show coexistence with rutile, muscovite and quartz, where these minerals dominate some examples. The roundness of pyrite points to grain transport under an-oxic conditions.

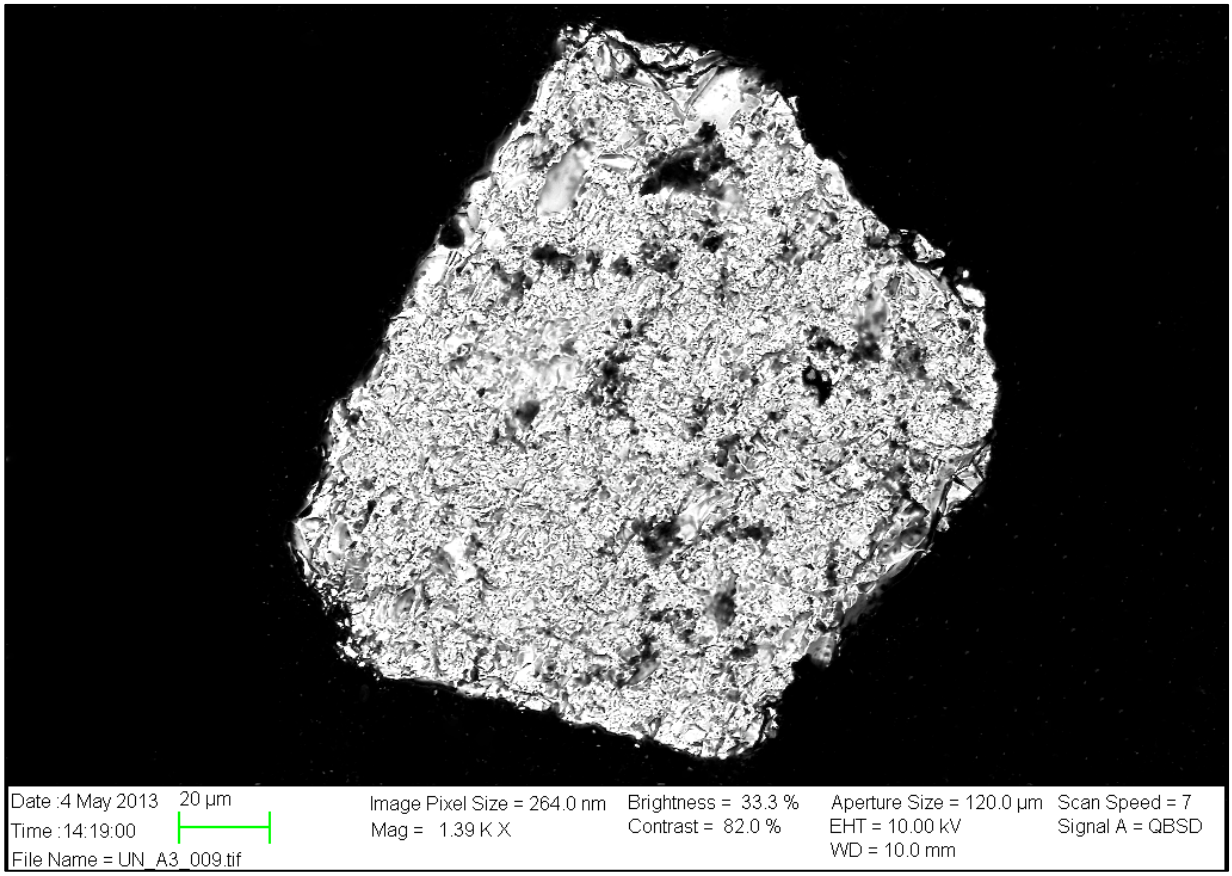

Figure 10 – Angular pyrite with rounded corner. BSE micrograph.

Other minerals:

Rutiles are encountered in association with quartz, and are generally angular with a size < 90 μm. Zircons are found as single grains and show mostly angular features, however some specimens reveal sub rounded – rounded shapes. The zircons are < 50 μm in size, were the rounded grains are < 30 μm in diameter. Bismite, nisnite and sillénite is found as single angular grains < 10 μm in length and with.

3.2.2.2 Zircon fraction

Zircon fraction is dominated by pyrite contributing with 80% of the sampled material, also zircons where found in smaller amounts with a total of 15%. Other heavy minerals observed are apatite, rutile, hematite/magnetite, barite, bravoite and horomanite. There were further an abundance of quartz and micas, typically muscovite and biotite, also albite and magnesium rich calcite, possibly dolomite, was encountered as lithoclasts.

Pyrite

The observed pyrite displayed sizes between 15 - 150 μm. There are many rounded samples with diameters in the lower part of the scale, however some larger rounded samples with diameter up to 60 μm were recorded. Angularity was present in the majority of the grains. These specimens were greater in size, some with cubical features and others with rounded to slightly rounded edges. The smaller specimens were typically found alone or together with mica, while the angular pyrites often coexisted with quartz.

Zircon

Zircon specimens yielded irregular and angular shapes. The irregular shaped were in greater quantities with sizes 5 - 30 μm, believed to be fragmented pieces. The angular specimens showed elliptical and cubical features, the sizes were greater, typical ranging between 10 - 60 μm. The zircon samples were usually found in solitude, with a minority coexisting together with quartz, also one specimen that encompassed a fluorapatite fragment (Figure 11). Also, a zircon grain reveling zonations was encountered, (Appendix E, Fig. E12)

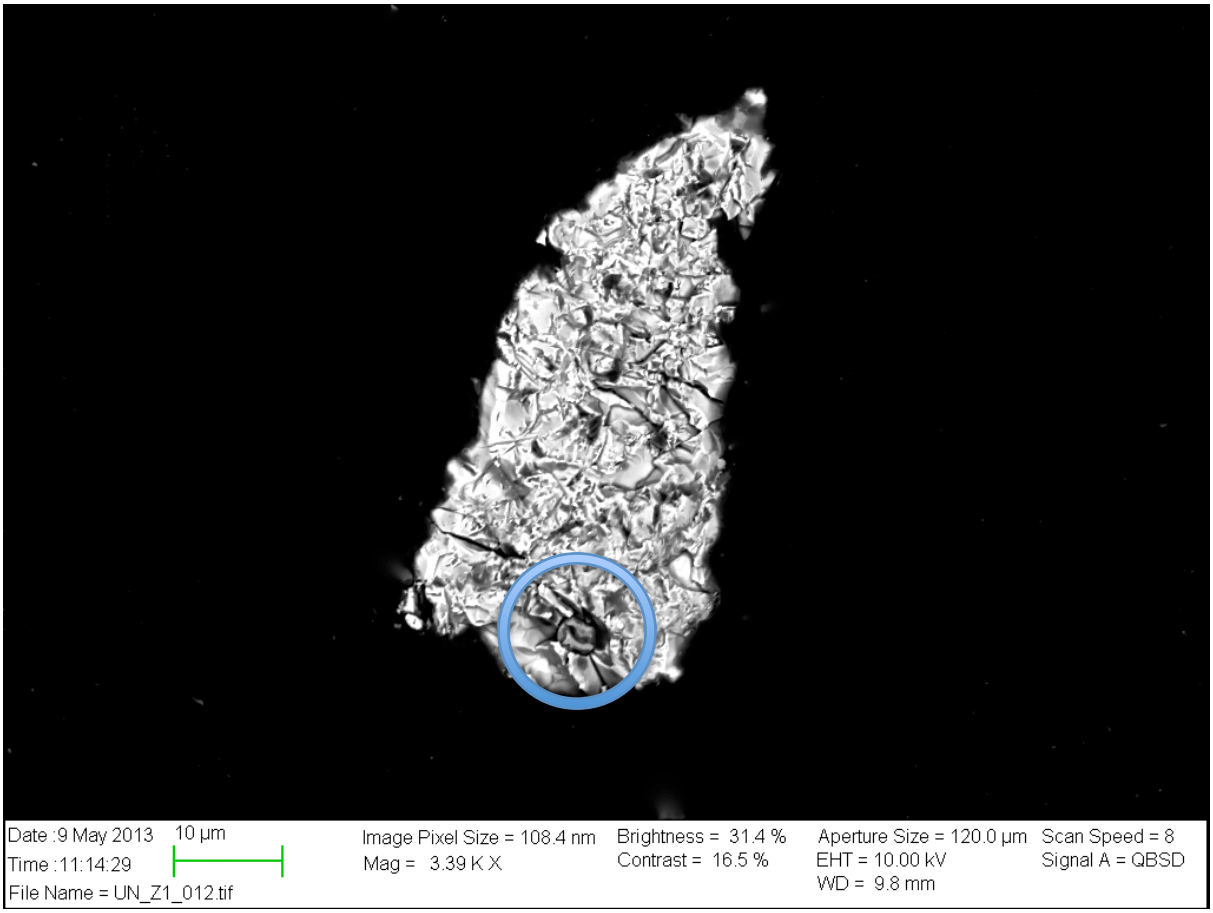

Figure 11 – Angular zircon grain surrounding a smaller grey rounded flurorapatite grain. BSE micrograph.

Other Minerals:

Most abundant of heavy minerals in lesser quantities was rutile, encountered as angular and irregular formed grains 5 – 50 μm in size, typically in coexistence with quartz. Also apatites were discovered. These were more rounded, and subjected to erosion. Compositional variations such as fluorapatite were recorded, however smaller in size and found inside zircons.

3.2.2.3 Magnetic fraction

The sampled fraction shows an abundance of fayalite (40%), pyrite (28%) and rutile (26%). Also recorded are magnetite, zircon, cuprite, apatite, and bismite, however, in small quantities and in cases only one specimen. Typically the heavy minerals were found in association with quartz and muscovite, which generally was in great abundance, also in fewer cases with feldspar.

Fayalite

Observed fayalites displayed angular grains with some indentations. The size ranged in size between 10 - 50 μm, were the smaller grains looked like eroded fragments. For all cases a coexistence with quartz was noticed and for some samples also with muscovite.

Pyrite

Pyrites exhibit sizes between 15 – 80 μm, typically with sharp angular edges. There are some examples were fractures around the edges have formed with indentations, possibly due to smaller fragments have broken loose.

Rutile

The rutiles are angular with sizes raging between 30 – 85 μm. There is observed rounded edges in some specimens, indicating transportation, and further, some cleavage is documented. The rutiles were often found in coexistence with quartz, and in minor quantities with zircon impurities. Also rutile was found surrounding an apatite grain.

Other Minerals:

Magnetites revealed angular features and generally small in size, $< 30\ \mu m$. Further there was encountered bismite and cuprite, both as single grains (Figure 12). The cuprite had angular edges with a size between 30 x 60 μm, which is in contrast to the much smaller bismite mineral. The bismites featured distinctive angular edges with a size $< 10\mu$m.

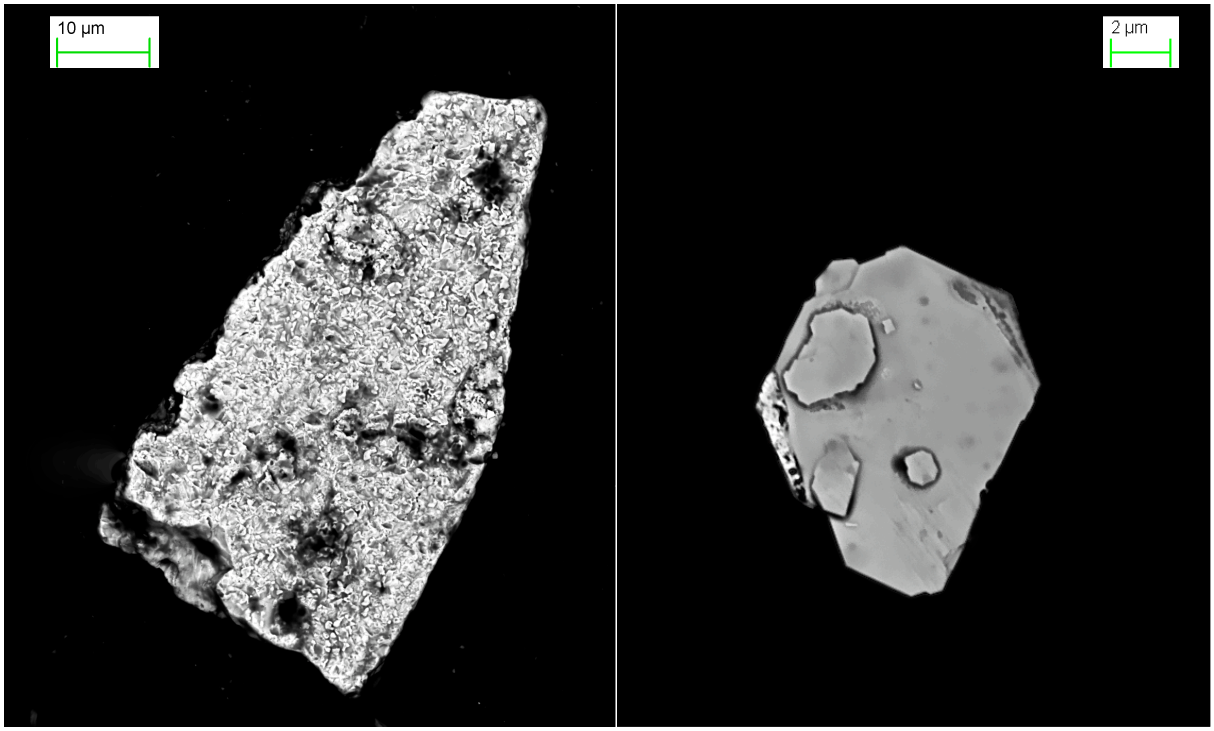

Figure 12 – Left: Angular cuprite. Right: Bismite mineral. BSE micrograph.

3.2.3 COMPILATION OF HEAVY MINERAL DATA

Fraction	Mineral (%, size, form)	Mineral (%, size, form)	Mineral (%, size, form)	Other:
Catavi Fm				
Apatite	Apatite (81%,40-100μm, rounded)	Zircon (11%,35-70μm, rounded)	Rutile (5%,30-70μm,Rounded)	Monazite, illmenite,
Zircon	Zircon (55%,25-160μm, various)	Rutile (43%,30-70μm,various)	Apatite (<2%, <35μm, rounded)	Titanite, pyrite
Magnetic	Fayalite (35%,50-120μm,various)	Monazite (15%, <65μm,sub-rounded/fragmented)	Magnetite (12%,35-150μm, rounded/fractured)	Zircon, rutile, Almadine,majorite, chromite
Uncía Fm				
Apatite	Pyrite (94%,30-150μm, various)	Zircon (<4%, <50μm, various)	Rutile (>2%,<90μm,various)	Bismite,nisnite, sillénite
Zircon	Pyrite (80%,15-150μm, various)	Zircon (15%, 5-60μm, various)	Rutile (>5%,5-50μm,angular)	Apatite, magnetite, barite, bravorite, horomanite
Magnetic	Fayalite (40%,10-50μm,angular)	Pyrite (28%, 15-80μm, angular)	Rutile (26%, 35-80μm, angular)	Magnetite, bismite, cuprite, zircon, apatite

Table 3 – Comparison of heavy mineral fractions.

Observations of the Catavi Formation reveal an abundance of apatite and zircon. A majority of the grains are detrital, while some specimens occur with few signs of erosion, (Figure 6) and (Figure 8). The grains are homogeneous regarding size, with some anomalies at both ends of the scale. Further, there was discovered fayalite and rutile in numbers. The grains show a various mix in regard of morphology, from angular to rounded and some irregular shapes. The fayalite grains are also found in a variety of sizes, while the rutile grains are more homogeneously distributed. Also monazite and magnetite minerals were documented, as

grains, fragments and impurities. Other heavy minerals found are ilmenite, pyrite, alamadine, majorite and chromite.

In the Uncía Formation, the fractions are dominated by pyrite, consisting of 67% of the total heavy mineral composition. Primarily the grains are geometrical, displaying sharp angular edges, indicating a short transportation before deposition. However, some show rounded to sub-rounded features indicative of erosion. Also, a variety regarding size is documented, suggesting different source material. Zircons are mostly found as irregular and rounded grains, however angular specimens are documented.

Angular grains dominate rutiles and fayalites, where fayalite grains show a more homogenous grain size than rutile grains. There are specimens that show rounded edges and appear as fragments in coexistence with quartz and mica. A very small amount of apatite was encountered, typically well rounded. However, compositional variations such as fluroapatite were recorded. Different compositions also encountered were bismite, bitumite, nisnite, sillénite, barite, bravorite, magnetite and cuprite.

The immature and poorly sorted compositions, in terms of size and roundness, suggest distribution from more than one source for both formations. The compositional variations when comparing the formations reveal distinct differences, suggesting different depositional sources and possibly conditions. The angular apatite grains from Catavi Formation are interesting since apatite is relatively unstable, (Figure 6). Conclusively, the samples from the Uncía Formation contain pyrite, even rounded grains, which means that the deposition and the transport happened under anoxic conditions. Pyrite is rare to absent in the Catavi Formation and points therefore to a radical change in the depositional setting although similar rock types have been described.

3.3 Geochemistry

3.3.1 MAJOR ELEMENT GEOCHEMISTRY

The sandstones of the Uncía and Catavi Formations reflect enrichment of silica or close to upper continental crustal composition (UCC after McLennan et al. 2006). They further show depleted values of Al_2O_3, K_2O and TiO_2. Shales in the Uncia Formation show relatively close to upper continental crustal composition in the silica concentration with some enriched specimens, which is in contrast to rocks from the Catavi Formation where a depleted trend dominates the values with some examples showing near UCC values. Fe_2O_3 values are low for sandstones and high for shales in the Catavi Formation, while in the Uncía Formation all values are enriched (> 5.4%). Further, there is a general depletion of MgO, CaO, P_2O_5 and MnO, where CaO is relatively low for all samples (< 0,5%) except CAT 10 with a value of 5.57%. However, there is a general enrichment of TiO_2 in shales for both formations.

3.3.2 ALTERATION

The Chemical Index for Alteration (CIA) for the sedimentary rocks is high for the Catavi Formation with values between 65 to 84 and an average of 75, while the older Uncía Formation displays an average of 81 with a smaller range from 77 to 87, (Table D 1, Appendix D) and is therefore stronger weathered. Samples are plotted in the A-CN-K diagram (after McLennan et al. 1990), (Figure 13), where the molar relationship of Al-Ca + Na-Ca is used to determine the alteration trends. The majority of the samples are divided into two groups of alteration, with the same trend towards kaolinitization, where the higher alteration has happened to the shales. There are two samples from the Catavi Formation (CAT 12 and 22) that deviate from the mentioned trend with values reflecting illite composition. K/Cs ratios (after McLennan et al. 1993) are below UCC values for all samples. However, the ratios

have variable values and when compared to post-Archean average Australian shale (PAAS, after Taylor and McLennan, 1985) the majority of the samples show values below this constant, with the exception of CAT 2 and 4. For the Uncía Formation the ratios are relatively close to PAAS for all samples. This supports the strong weathering trend by the CIA.

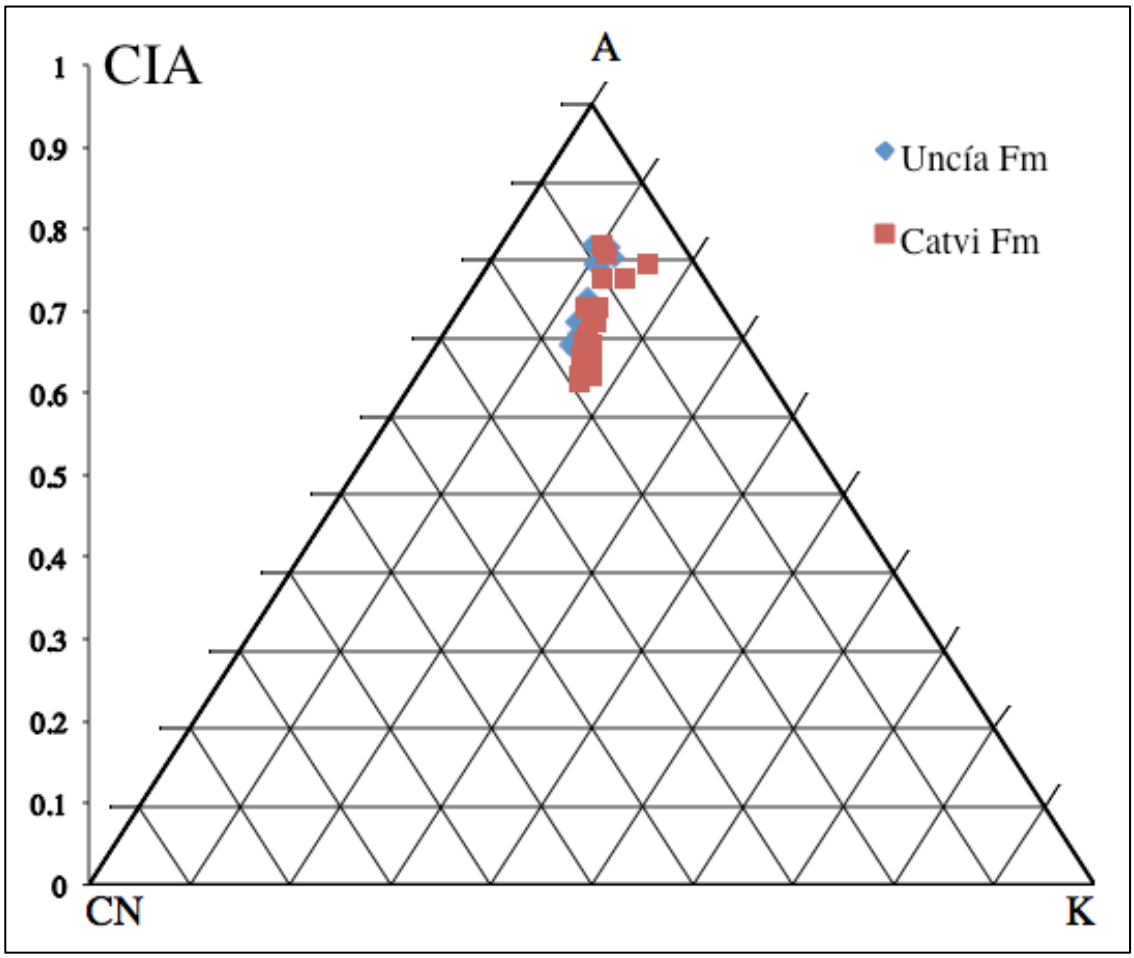

Figure 13 – A-CN-K diagram (after McLennan et al. 1990)

3.3.3 Trace elements and Rare Earth Elements

3.3.3.1 Composition

Using selected trace element geochemistry, classification of the sedimentary composition can be determined using ratios of Zr/Ti versus Nb/Y, as these elements are strongly immobile (after Winchester & Floyd, 1977). Rock samples from the Catavi Formation point to a mainly intermediate composition. Shales are close to upper continental crustal values (UCC after McLennan et al. 2006), while sandstones appear to be more felsic. The samples from the Uncía Formation are more homogeneously distributed displaying a rhyolitic composition, however, a division between sandstone and shale is present. The sandstones have a higher Nb/Y concentration compared to the shales, but both are comparable in Zr/Ti ratios.

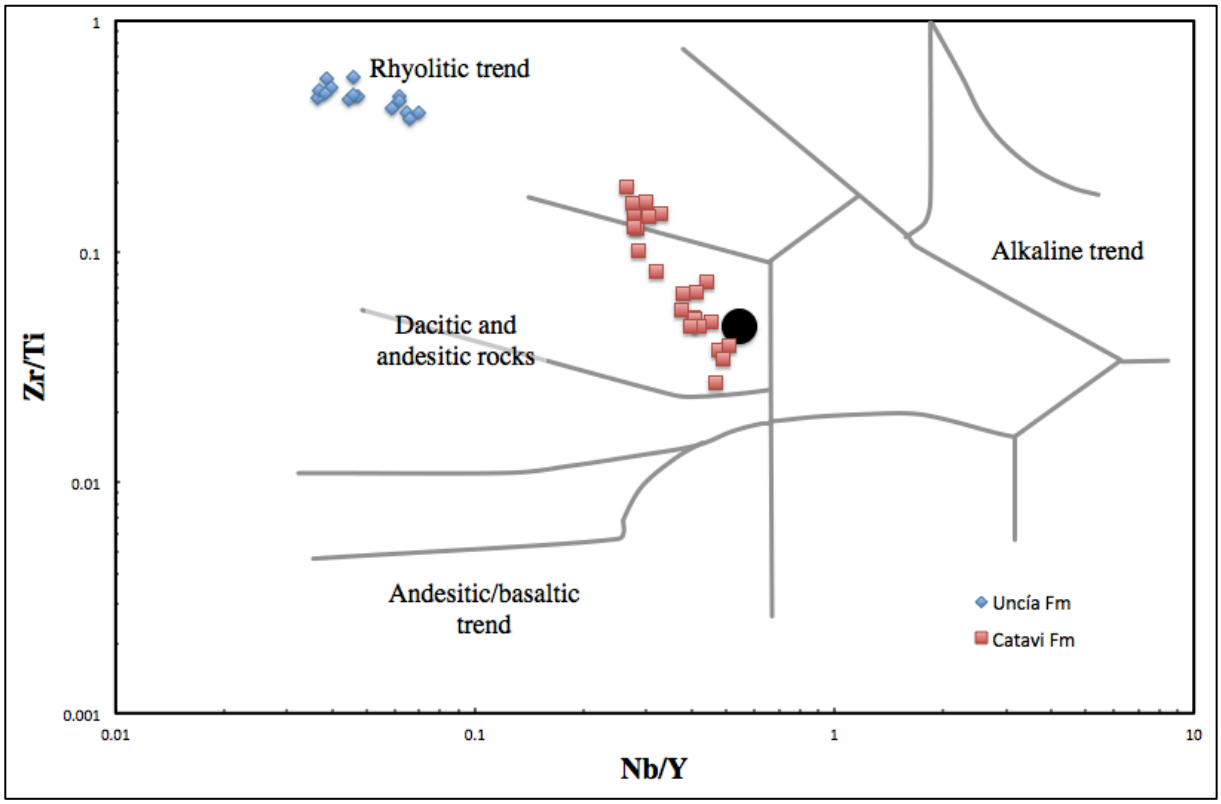

Figure 14 – Geochemical plot after Winchester and Floyd (1977) to demonstrate the general composition of the samples. The black circle denotes typical Upper Continental Crust composition (after McLennan et al., 2006).

Trace elements, such as high field strength elements Th, Sc and Zr and REE, are particularly useful for provenance analysis due to their insolubility and immobility under surface conditions (Zimmermann & Bahlburg, 2003). Also, because their typical behavior during fractional crystallization, weathering and recycling, they maintain the original characteristics of the source rock in the sedimentary record (e.g Taylor & McLennan, 1985; Bhatia & Crook, 1986; McLennan, 1989; McLennan et al., 1993; Roser et al., 1996). Selected elements and Rare earth elements (REE) of the sampled rocks are normalization to typical UCC (after McLennan et al., 2006), (Figure 15). In this diagram elements have been listed from right to left in order of increasing ocean residence times, such that elements to the right are generally stable (low residence time) and quantitatively transferred to the depositional area, whereas those to the left are generally mobilized during weathering (long residence time) and then selectively adsorbed from solution at the site of deposition (Floyd et al., 1990). Both formations have similar patterns reflecting comparable source compositions characterized by marked negative Sr and P and positive Cs anomaly. Most of the sandstones from both formations show depletion in compatible elements such as Cr, Ni, V and Sc, but less pronounced for Nb and Ta, which is more evident in Figure 16, were average values from each rock type within the formations is shown. The stable element group from Yb – Th indicates that the source was of generally upper continental crust composition, where shales exhibit a minor enrichment and the Catavi Formation sandstones show positive Zr and Hf anomalies.

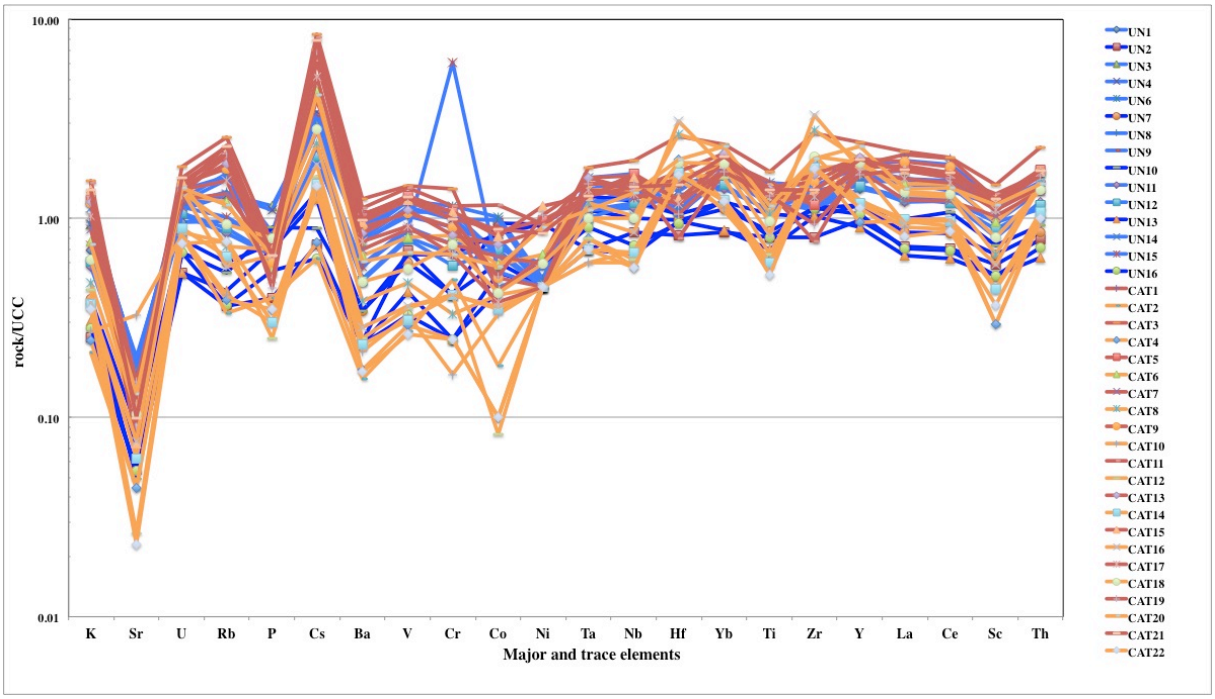

Figure 15 – Normalisation of major and trace elements of the Catavi and Uncía Formation samples to typical Upper Continental Crust composition (after McLennan et al., 2006) in a plot after Floyd and Leveridge, 1987.

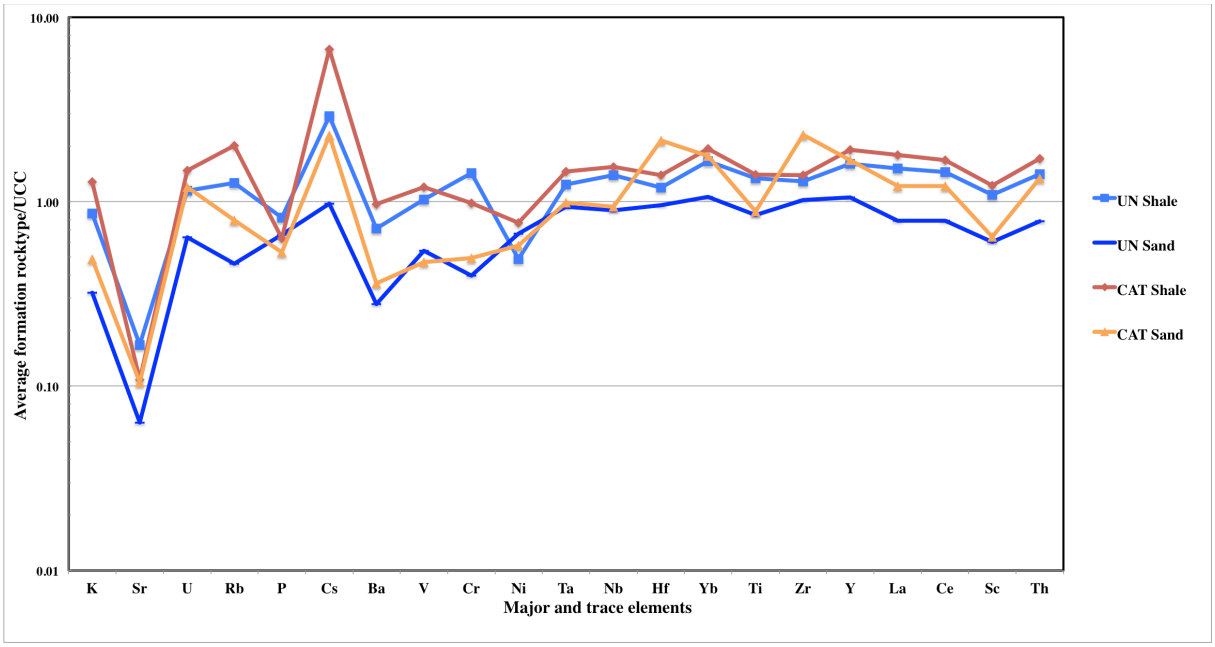

Figure 16 - Normalisation of major and trace elements of the average rock type from Catvi and Uncía Formation samples to typical Upper Continental Crust composition (after McLennan et al., 2006) in a plot after Floyd and Leveridge, 1987.

3.3.3.2 Rare Earth Elements

Rare Earth Elements (REE) pattern can reveal information about the composition of sedimentary rocks. REE for samples normalized to chondritic values are shown in (Figure 17). The samples from the Uncía and Catavi Formations show relatively homogeneous shapes indicative of a retro arc setting. Shales from both formations have greater values compared to the sandstones, with the exception of the sandstones CAT 6, 18 and 20, which plot intermediate to the shales from both formations. Furthermore, the LREE show a moderate enrichment with La_N/Yb_N ratios of 5 to 10. All samples comprise a modest negative Eu/Eu* anomaly between 0.38 and 0.81 (mean = 0,57; SD = 0,08), (Appendix D, Table D.1).

The samples from the Uncía Formation have an enrichment of Yb compared to the Catavi Formation, where the shales show a stronger enrichment than the sandstones. However, averaging values from both localities one clearly see that they plot similar to values of PAAS, (Figure 18).

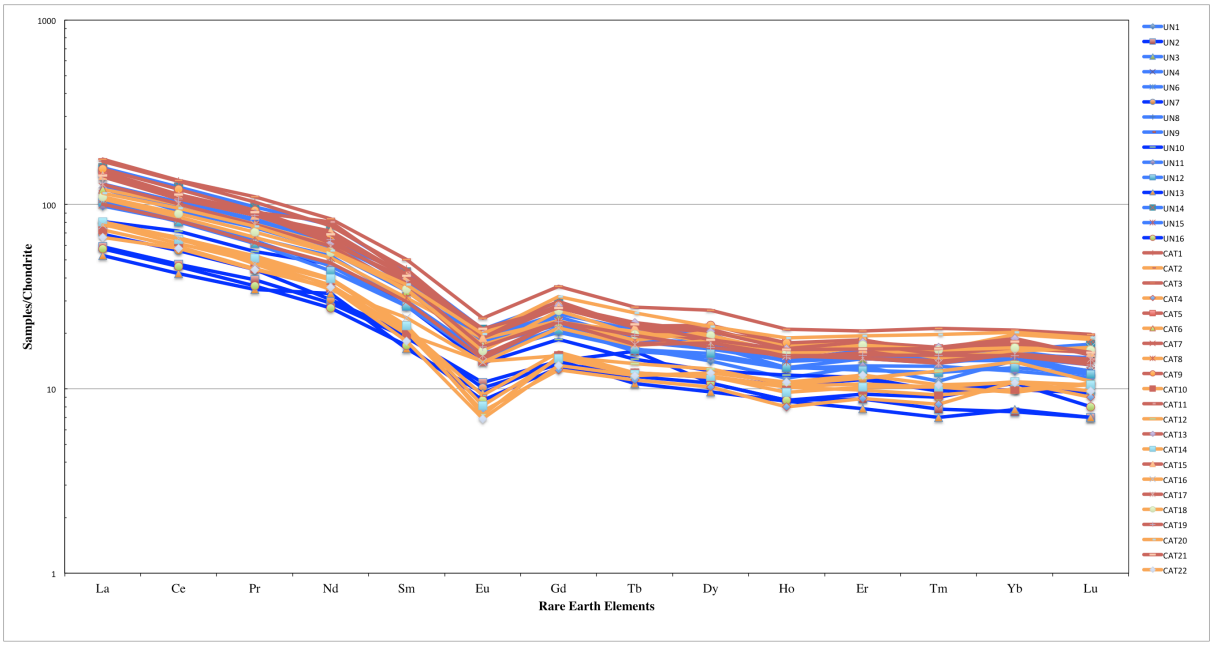

Figure 17 – Rare earth elements from Uncía and Catavi Formation normalized to chondritic values (after Taylor and McLennan, 1985)

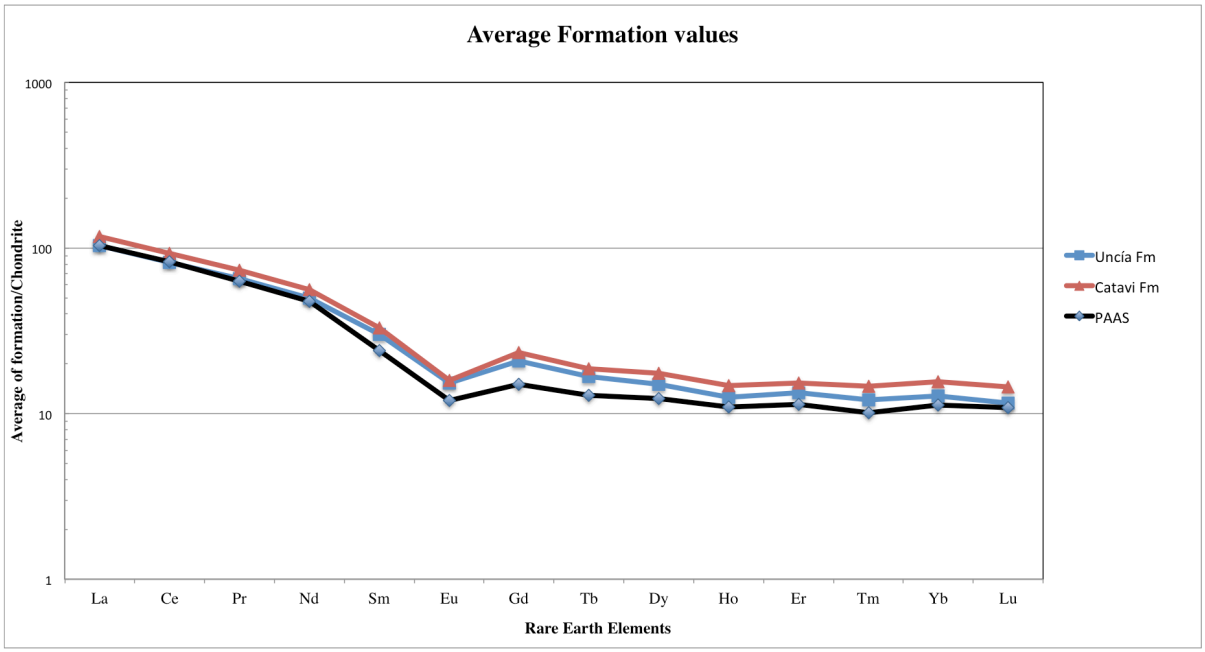

Figure 18 - Rare earth elements from average formation values from Uncía and Catavi Formation normalized to chondritic values (after Taylor and McLennan, 1985) demonstrate the upper crustal nature of most of the detrital material.

3.4 Provenance and palaeotectonic setting

The origin of the detritus in terms of the composition of the source mix is often successfully demonstrated with the ratios Th/Sc and Zr/Sc (after McLennan et al., 1990). In Figure 19, the Th/Sc ratio expresses the grade of fractionation while Zr/Sc values indicate the degree of reworking of the detritus leading to enrichment of the stable zircon mineral. Samples from both formations show similar characteristics with Th/Sc values above typical UCC (<0.79). However, samples from the Uncía Formation have the lowest Th/Sc ratios, and for both rocktypes, shales and sandstones, very similar ones. Only the shales of the Catavi Formation have similar low Th/Sc values around 1 but the sandstones comprise elevated values up to 3. These samples are also the strongest recycled ones with the highest Zr/Sc ratios up to 100.

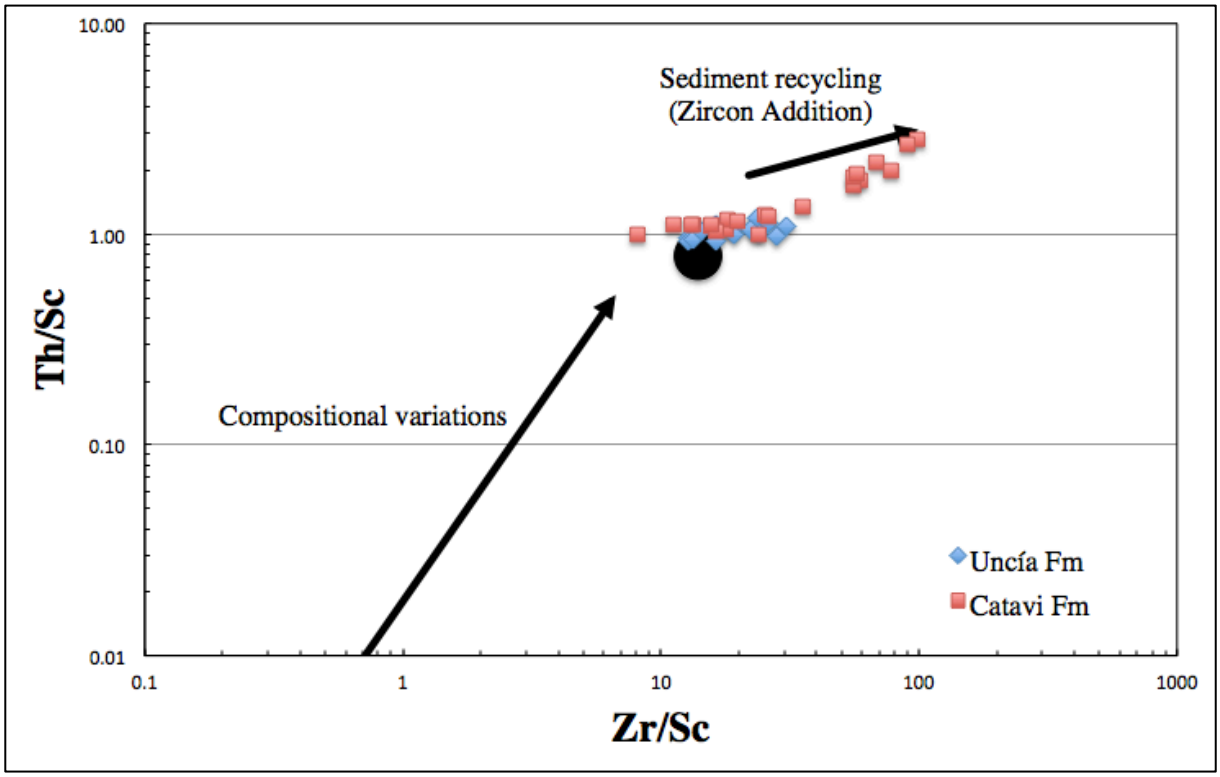

Figure 19 – Th/Sc versus Zr/Sc ratios (after McLennan et al., 1990), black circle denotes typical UCC (after McLennan et al., 2005)

The palaeotectonic setting of the detrital mix can be determined when using La/Sc and Ti/Zr ratios (after Bhatia and Crook, 1986), (Figure 20). However, it is necessary to mention that these ratios reflect the mixed detritus and can therefore as well reflect the composition of the detritus. The samples in this diagram plot differently and it is clear that their detritus is composed of different sources. The shales from the Uncía Formation are clustered and show higher Ti/Zr ratios, while the sandstones are more scattered with single samples with higher La/Sc ratios. The shales from the Catavi Formation have a similar trend as the Uncía shales, however, with a larger scatter in the Ti/Zr ratios. Both samples are entangled, and somewhat scattered, and point to their sedimentary composition to a mix between a continental island arc and active continental margin provenance. However, for sandstones in the Catavi Formation ratios of La/Sc > 4 and Ti/Zr > 7 are therefor prone to a passive rift margin provenance.

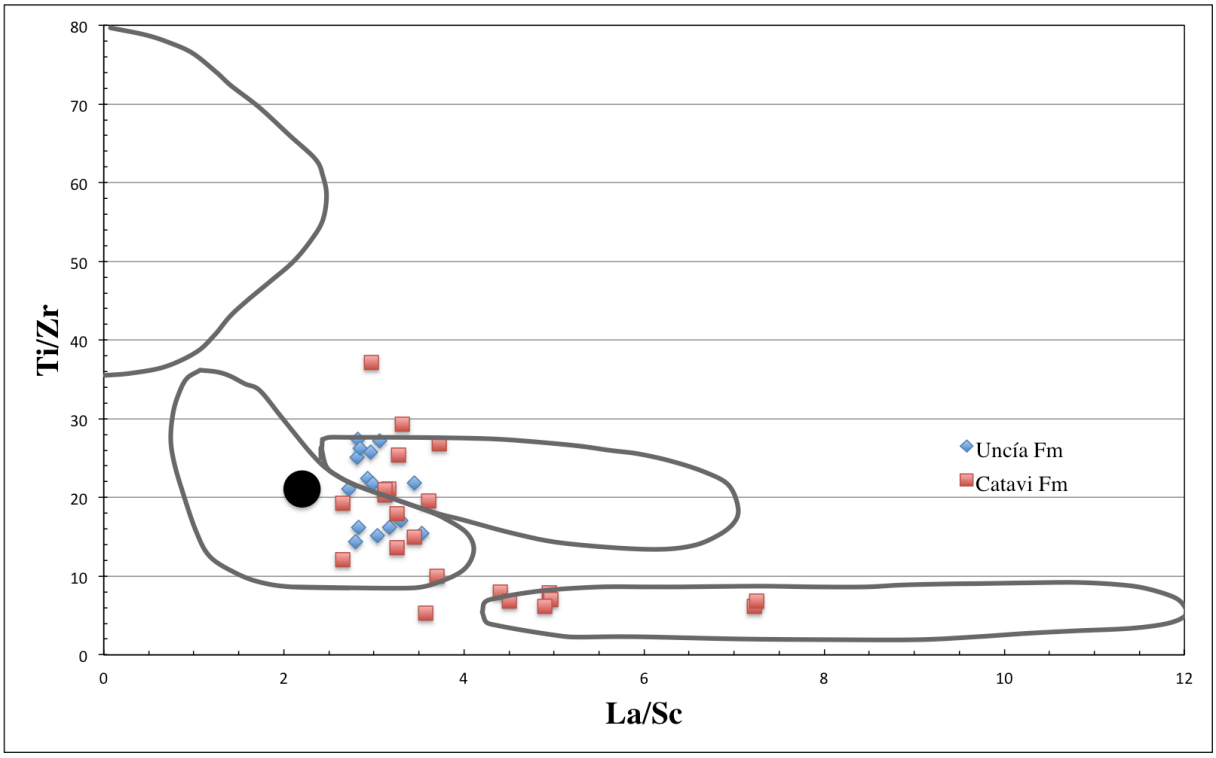

Figure 20 – Ti/Zr versus La/Sc diagram (after Bhatia and Crook, 1986), black circle denotes typical UCC (after McLennan et al., 2005)

3.5 Organic Carbon

Both formations are disappointingly very low in total carbon, (Table 4), and therefore no source rock for younger formations. Alternatively, organic matter might have been stored but during the different orogenic events, the hydrocarbons may have been migrated.

	Organic C %	**Total C** %
UN 1	0.18	0.2
UN 6	0.49	0.63
UN 8	0.45	0.56
UN 15	0.28	0.39
UN 16	0.09	0.17
CAT 4	0.03	0.06
CAT 6	0.17	0.22
CAT 14	<0.02	0.44
CAT 20	0.12	0.28

Table 4 - Total carbon and organic carbon in the Catavi and Uncía Formations. Shales are in cursive letters.

Migration of hydrocarbons is less likely as some samples of the Cancañiri Formation still have some % of organic carbon (Mehus, 2013). It seems rather that after mass extinctions only few species have been re-developed and a scarcity of organic matter was the general case. The extremely low concentrations of organic matter is exceptional and not expected.

3.6 Discussion and Implication

Petrological and heavy mineral results show a distinct difference in mineral composition from Uncía and Catavi Formation. The Catavi Formation presents large amounts of zirconium and apatite, with a majority of rounded grains. Furthermore, apatite grains are mainly rounded, however highly angular samples were detected, (Figure 6), which is interesting due to its unstable nature. The results point to a composition from two sources with different lengths of transportation.

Uncía Formation is texturally immature with quartz as the major component, with secondary hematite intrusion and elongated muscovites. Heavy minerals reveal a high abundance of pyrite, with low amounts of zircon and rare specimens of apatite, pointing to a restricted source. The pyrites are bimodal, the largest group feature angular grains larger in size compared to those with a rounded morphology. This points to a deposition and even transport under an-oxic conditions. This situation did not enhance very much the abundance of organic carbon in the Uncía Formation, although values are in fact higher than in the underlying rocks, (Table 4). However, the general visual features are scattered for nearly all heavy minerals, suggesting input from different sources, with different lengths of transportation, or in regard of the quartz, cannibalization of a quartz rich source in near proximity, possibly the

underlying Cancañiri Formation. From the same source also the rounded pyrite might have been eroded.

In regard of geochemistry, the Catavi Formation is characterized by a difference for nearly all geochemical proxies for shales and sandstones. The latter are close to a rhyolitic composition while the former are intermediate, (Figure 14). This can be an effect of reworking as such that the source of these rocks has been similar and comparable with the shales but the sandstones have been reworked stronger and are therefore quartz-richer and show higher Zr/Sc and La/Sc ratios, (Figure 19) and (Figure 20). The change in provenance also is accompanied with a change in the palaeoenvironment as the detrital pyrite disappears and even less organic carbon is stored. Therefore the Catavi Formation might indicate an already very well oxygenated basin, receiving the detrital components of the surrounding sources and not from underlying rocks. Samples of the Uncía Formation are different, as both, shales and sandstones are similar in their geochemical trends. Regarding their Zr/Ti ratios and Nb/Y values the rocks are similar to rhyolites, but in most of the other plots the rocks show similarities to a typical UCC without a recycling component.

Hence, both formations are different in their provenance and in their mechanisms of storing provenance information. Sorting did not play a role in the Uncía Formation rocks and point to the recycling of a quartz-rich source in proximity, while the major source of the Catavi Formation has been less fractionated then the source of the Uncía Formation and had been recycled in the sandstones. This point either to a source further away from the sink area or to a different facies for the quartz-rich rocks of the Catavi Formation in comparison to the Uncía Formation.

In Table 5, geochemical values in red indicate an arc derivation for detrital mixes, and orange show relative close to arc values. Most of the samples show proxies of a continental

arc component mixed with a felsic source. Sandstones show a stronger arc relationship than shales, where the Uncía Formation sandstones have the strongest arc signature.

Sample	SiO2	La/Sc	Th/Sc	Zr/Sc	Ti/Zr	Eu/Eu*	LaN/YbN	TiO2	Nb	Ta
UN1	66.77	2.93	0.93	16.27	22.39	0.61	7.23	0.79	14.3	1.1
UN2	76.59	2.73	1.06	19.18	21.1	0.6	7.83	0.54	10.2	0.7
UN3	62.34	2.82	0.96	12.71	27.41	0.64	8.56	0.93	16.7	1.2
UN4	62.72	3.06	0.94	12.69	27.24	0.56	9z.78	0.98	18.5	1.3
UN6	61.39	2.81	1.06	13.76	25.12	0.58	8.41	0.98	20.1	1.6
UN7	77.11	2.83	1.02	23.8	16.23	0.59	6.98	0.58	12.1	1.1
UN8	63.24	2.85	0.94	13.28	26.24	0.61	8.19	0.93	16.6	1.1
UN9	62.94	2.96	1.04	14.25	25.77	0.56	8.01	0.98	18.8	1.4
UN10	71.58	2.99	1	19.26	21.79	0.58	7.54	0.7	14.8	1.3
UN11	71.1	3.3	1.19	23.66	17.04	0.63	7.86	0.74	13.5	1.1
UN12	71.16	3.18	1.05	22.17	16.23	0.61	7.9	0.72	14.4	1
UN13	79.83	2.8	0.99	27.96	14.4	0.65	6.86	0.47	7.9	0.7
UN14	62.39	3.45	1.11	16.29	21.86	0.59	9.7	1.01	19.2	1.4
UN15	69.74	3.53	1.14	26.26	15.45	0.6	8.38	0.88	15.2	1.2
UN16	81.94	3.04	1.1	30.54	15.14	0.57	5.35	0.54	8.8	0.9
CAT1	61.75	3.72	1.12	13.41	26.82	0.54	9.97	1.02	19.7	1.6
CAT2	88.05	7.23	2.8	98.03	6.12	0.51	8.17	0.4	8.2	0.6
CAT3	58.11	3.26	1.24	25.37	13.59	0.57	8.44	1.15	23.5	1.8
CAT4	88.23	7.25	2.65	89.93	6.83	0.43	7.18	0.41	6.9	0.8
CAT5	59.25	3.28	1.12	13.05	25.41	0.57	8.53	0.94	20.2	1.3
CAT6	71.35	3.45	1.21	26.25	14.93	0.59	7.31	0.85	16.8	1.4
CAT7	67.8	2.65	1.06	17.77	19.28	0.56	6.53	0.8	15.4	1.4
CAT8	77.76	4.4	1.81	58.64	7.95	0.7	5.43	0.7	12.3	1.2
CAT9	63.96	3.61	1.16	18.21	19.54	0.56	9.07	0.95	18	1.5
CAT10	74.76	4.5	1.72	55.52	6.84	0.81	7.33	0.38	7.2	0.6
CAT11	48.67	2.97	1.01	8.15	37.19	0.59	9.56	0.91	19.1	1.3
CAT12	84.46	4.95	1.87	55.8	7.88	0.38	5.72	0.44	7.5	0.8
CAT13	63.17	3.26	1.16	19.66	17.91	0.58	7.51	0.94	16.8	1.6
CAT14	81.72	4.97	1.95	57	7.01	0.43	7.38	0.4	8.1	0.7
CAT15	54.22	3.12	1.09	15.64	20.3	0.55	8.58	0.9	19.2	1.3
CAT16	82.17	3.58	2	78.44	5.25	0.63	4.84	0.55	10.3	1
CAT17	68.12	3.17	1.04	16.28	21.11	0.52	8.31	0.86	16	1.4
CAT18	74.83	3.7	1.36	35.52	9.97	0.54	6.59	0.65	12	1
CAT19	59.41	3.31	1.11	11.11	29.35	0.54	9.45	0.87	18	1.5
CAT20	72.76	2.66	1.01	23.8	12.12	0.6	5.68	0.77	16.2	1.1
CAT21	60.01	3.12	1.11	15.62	21	0.61	7.96	0.93	17.3	1.3
CAT22	87.93	4.9	2.18	68.04	6.17	0.43	6.13	0.35	6.8	0.7
ARC*		< 3	< 0.81	< 10	> 20	1	< 6	< 0.68	< 12	< 1

Table 5 – Geochemical proxies for all samples from Uncía and Catavi Formations. Yellow markings indicate sandstones, red indicate arc related and orange less fractionated values than typical arc (ARC) after McLennan et al. (1990, 1993).

This might point to the erosion of a previously exposed or still covered arc related successions slightly older than the Cancañiri Formation as syn-volcanic arc formations in Peru, to the north, or Argentina, towards the south, have Middle Ordovician ages (Zimmermann and Bahlburg, 2003; Bahlburg et al., 2006).

4.0 PETROLEUM SIGNIFICANCE

In the search of a mechanism that explains the high abundance of Silurian shale rocks as observed in Europe (Craig et al., 2009) or to observe the response of sea level changes after a glaciation with the bury of massive organic matter we started the research project in Bolivia. Observed black shales shall be the source for massive hydrocarbons in Bolivia. Black shales and other fine-grained rocks in Bolivia did not show any significant organic contents although their color pointed to such a possibility and their deposition had been under anoxic conditions, identified by detrital pyrite. Hence, the dark color only reflects the abundance of base metals (Mehus, 2013) and here the occurrence of rare base metal rich minerals. The only explanation so far is that in this region of Gondwana after the Hirnantian mass extinction, life did not recover as rapid as in other areas like northern Gondwana (Craig et al., 2009). Hence, source rocks for the massive hydrocarbon reservoirs in Bolivia are most likely not of Lower Palaeozoic age.

5.0 CONCLUSION

In this project post- Hirnantian rocks from Bolivia close to La Paz have been studied. The two exposures are located in the Eastern Cordillera consisting of the Catavi Formation and the Uncía Formation. The formations studied are composed of siliciclastic rocks deposited during late Llandovery to Pridoli with a stratigraphic relationship to the older Cancañiri formation consisting of Hirnantian glacial deposits and black shales, supposedly a source for organic material as in other parts of the Gondwana margin.

Applied methods focusing on composition using quantitative tools have provided result characterizing their provenance, source and paleohistory, and how Bolivia have responded to deglaciation in terms of organic rich rocks.

Petrological and heavy mineral results show a distinct difference in mineral composition from the Uncía and Catavi Formation. Where the Catavi Formation reveals large amounts of zirconium and apatite, with a majority of rounded grains. Compared to the Uncía Formation where pyrite dominates the heavy mineral fraction, showing a record of rounded samples, let one assume an environment with low abundance of oxygen. Further, the provenance of the Uncía Formation point to a source or sources relatively close to the depositional areas as sorting did not play a role, due to the similar trace element signature in sandstones and shales. However, organic matter is absent or has never been preserved. As the sandstones of this formation contain a variety of arc-related geochemical proxies one source might have been a Mid Ordovician succession, previously exposed and covered, in proximity, and/or the underlying pyrite-rich Cancañiri Formation. The depositional environment changes towards the younger rocks of the Catavi Formation, with less preserved pyrite and even less organic carbon. The sources for this formation might have been more variable but point to longer

transportation of the grains. Therefore the Catavi Formation might indicate an already very well oxygenated basin, receiving the detrital components of the surrounding sources and not from underlying rocks. The absence of any characteristics for larger organic matter, with even absence of common graptolites in the shales, point to deposition under partly anoxic conditions but without abundant organic matter.

Hence, it seems that the post-Hirnantian faunas did not recover until the Uncía Formation in contradiction to northern Gondwana successions, today deposited in Europe where Silurian rocks are rich in organic matter. This implies for Bolivia that hydrocarbon reservoirs have been sourced from other rocks and that the black shales of the Cancañiri Formation is not a result of organic matter but rather reflects an abundance of rare base metal rich minerals. It seems that after the mass extinctions only few species have been re-developed and a scarcity of organic matter was the general case. The extremely low concentration of organic matter is exceptional and not expected. Hence, source rocks for the massive hydrocarbon reservoirs in Bolivia are most likely not of Lower Palaeozoic age.

REFERENCES

Armstrong, H. A. et al., (2005) Origin, sequence stratigraphy and depositional environment of an upper Ordovician (Hirnantian) deglacial black shale, Jordan. *Palaeogeography, Palaeoclimatology, Palaeoecology,* Vol.220, pp. 273-289.

Baby, P., Sempere, T., Oiler, J., Barrios, L. and **Marocco, R.** (1990) Un bassin en compressiond'Lge oligo-miocene dans le sud de I'Altiplano bolivien. Cornpies *Rendues de 1'Academie des Sciences de Puris Se'rie II* Vol.311, pp.341-347.

Bahlburg, H., Carlotto, V. and **Cárdenas, J.,** (2006) Evidence of Early to Middle Ordovician arc volcanism in the Cordillera Oriental and Altiplano of southern Peru, Ollantaytambo Formation and Umachiri beds, *Journal of South American Earth Sciences* Vol. 22, pp. 52–65

Craig, J., Thurow, J., Thusu, B.,Whitham, A. and **Abutarruma, Y.** (2009) Global Neoproterozoic Petroleum Systems: The Emerging Potential in North Africa. *Geological Society, London, Special Publications*, Vol. 326, pp. 1–25.

Floyd, P.A. and **Leveridge, B.E.** (1987) Tectonic environment of the Devonian Gramscatho basin, south Cornwall: Framework mode and geochemical evidence from turbidite sandstones. *J. Geol. Soc. London*, Vol. 144, pp. 531-542.

Fricke, E., Ch. Samtleben, H., Schmidt-Kaler, H., Uribe and **Voges, A.** (1964) Geologische Untersuchungen im zentralen Teil des bolivianschen Hochlandes nordwestlich Oruru, *Geol. Jb.,* Vol. 83, pp.1-30.

Gubbels, T.L., Isacks, B.L. and Farrar, E., (1993) High-level surfaces, plateau uplift, and foreland development, Bolivian Central Andes. *Geology,* Vol. 21, pp. 498-695.

Hérail, G., Baby, P., Oller, J., López, M., López, O., Salinas, R., Sempere, T., Beccar, G. and **Toledo, H.,** (1990) Structure and kinematic evolution of the sub-Andean thrust system of Bolivia, *First International Symposium on Andean Geodynamics, Grenoble: Paris, Editions de l'Orstom*, pp. 179–182.

Isacks, B. L., (1988), Uplift of the central Andean plateau and bending of the Bolivian orocline. *Journal of Geophysical Research*, Vol. 93, pp. 3211–3231.

Jaillard, E., Hérail, G., Monfret, T., Díaz-Martínez, E., Baby, P., Lavenu, A., and **Dumon, J. F**., (2000) Tectonic evolution of the Andes of Ecuador, Peru, Bolivia and Northernmost Chile. *Tectonic Evolution of South America*, pp. 481–559.

Kley, J., Miller, J., Tawackloi, S., Jacobshagen, V. and **Manutsoglu, E.,** (1997) Pre- Andean and Andean- age deformation in the Eastern Cordillera of Southern Bolivia. *Journal of South American Earth Sciences,* Vol. 10, pp. 1-19.

Koeberling, F.R., (1919) Informe sobre la geología de las propoedades mineras de la Comañia Estañifera de LLallagua,- *Informer intero Cia.Estañifera Llallaugua.*

Mange, M. A. and **Maurer, H. F. W.** (1992) Heavy minerals in colour. *Chapman & Hall.*

Martínez, E.D-. and **Grahn, Y., (2007)** Early Silurian glaciation along the western margin of Gondwana (Peru, Bolivia and northern Argentina): Palaeogeographic and geodynamic setting. *Palaeogeography, Palaeoclimatology, Palaeoecology* Vol. 245, pp.62–81

McLennan, S.M., Taylor, S.R., McCulloch, M.T. and **Maynard, J.B.** (1990) Geochemical and Nd-Sr isotopic composition of deep-sea turbidites: Crustal evolution and plate tectonic associations. *Geochim. Cosmochim. Acta*, Vol.54, pp. 2015-2050.

McLennan, S. M., Hemming, S., McDaniel, D.K. and **Hanson, G.N.** (1993) Geochemical approaches to sedimentation, provenance and tectonics. *Processes controlling the composition of clastic sediments (Eds M.J. Johnsson and A. Basu), Geol. Soc. Am. Spec. Pap.,* Vol. 284, pp. 21-40.

McLennan, S.M., Taylor, S.R. and **Hemming, S.R.** (2006) Composition, differentiation, and evolution of continental crust: constrains from sedimentary rocks and heat flow. *Brown, M., Rushmer, T. (Eds.), Evolution and differentiation of the continental crust*, pp.92-134.

McQuarrie, N., Horton, B.K., Zandt, G., Beck, S., and **DeCelles, P.G.,** (2005), Lithospheric evolution of the Andean fold-thrust belt, Bolivia, and the origin of the central Andean plateau. *Tectonophysics*, Vol. 399, pp. 15 – 37.

Mehus, T (2013) From Cold to Hot: Post- Hirnantian Sedimentary Basins in Bolivia- A Source Rock for Hydrocarbon Deposits in The Andes? – A Case Study of the Cancañiri Formation. *Unpublished manuscript*

Murray, B. P., Horton, B. K., Matos, R. and **Heizler, M.T** (2010) Oligocene–Miocene basin evolution in the northern Altiplano, Bolivia: Implications for evolution of the central Andean backthrust belt and high plateau. *Geological Society of America Bulletin,* Vol. 122, no. 9-10, pp. 1443-1462

Nesbitt, H.W. and **Young, Y.M.,** (1982) Early Proterozoic climates and plate motions inferred from major element chemistry of lutites. *Nature*, Vol. 299, pp. 715-717.

Oller, J., and **Sempere**, **T.,** (1990) A fluvio-eolian sequence of probable Middle Triassic–Jurassic age in both Andean and sub-Andean Bolivia, *First International Symposium on Andean Geodynamics, Grenoble: Paris, Editions de l'Orstom, pp. 237–240.*

Pettijohn, F. R., Potter, P. E. and **Sieve, R.,** (1987) Sand and sandstone. *Springer Verlag*

Potts, P. J., (1987) A handbook of silicate rock analysis. *Chapman and Hall*. pp.286-381.

Schönian, F., Egenhoff, S. O., Marcinek, J. and **Erdtmann, B. D.,** (1999) Glaciation at the Ordovician–Silurian boundary in southern Bolivia. *Geologica* Vol.43, pp.175–178.

Sempere, T., (1994) Kimmeridgian? to Paleocene Tectonic Evolution of Bolivia. *Cretaceous Tectonics of the Andes: Earth Evolution Sciences Monograph Series (Eds: J.A. Saltity)*, pp. 168-212.

Sempere, T., (1995) Phanerozoic evolution of Bolivia and adjacent regions, *Petroleum basins of South America: AAPG Memoir* Vol. 62, pp. 207–230.

Sempere, T., G. Hérail, J. Oller, and **P. Baby**, (1989) Geologic structure and tectonic history of the Bolivian orocline, *28th International Geological Congress, Extended Abstracts, Washington, D.C.,* Vol. 3, pp. 72–73.

Sempere, T., Herail, G., Oiler, J. and **Bonhomme, M.,** (1990) Late Oligocene-early Miocene major tectonic crisis and related basins in Bolivia. *Geology* Vol. 18, pp.946-949.

Sempere, T., Hérail, J., Oller, J., Baby, P., Barrios, L. and **Marocco, R.,** (1990) The Altiplano: a province of intermontane foreland basins related to crustal shortening in the Bolivian orocline area, *First International Symposium on Andean Geodynamics, Grenoble: Paris, Editions de l'Orstom,* pp. 167–170.

Suaréz Soruco, R., Estenssoro, S, C., and **Zapata, C, M., (2000)** Revista Tecnica De Yacimentos Petrolliferos Fiscales Bolivianos *Compendio de Geologia de Bolivia*, Vol 18 (1-2), pp. 39-76.

Suarez-Riglos, M., Dalenez-Farajat, A. and **Perez, H.,** (1996) Contenido fauìstico del Lludloviano-Pridolino de Huari, Oruro (Altiplano de Bolivia). *Memorias del XI Congreso Geológica de Bolivia (Santa Cruz),* pp. 214-225.

Tankard, A, J., Soruco R, S., and Welsink H, J., (1995) Petroleum Basins of South America, *AAPG Memoir*, Vol. 62. pp. 423-558.

Turner, G. and **Morton, A.C**. (2007) The effect of burial diagenisis on detrital heavy mineral grain surface textures. *Heavy minerals in use, Developments in sedimentology*, Vol. 58, pp. 393-412.

Tyson, R.V., (1996) Sequence-stratigraphical interpretation of organic facies variations in marine siliciclastic systems: general principles and application to the onshore Kimmeridge Clay Formation, UK. *Sequence Stratigraphy in British Geology*. *Geological Society, London, Special Publication,* Vol. 103, pp. 75–96.

Tyson, R.V. and **Pearson, T.H.,** (1991) Modern and ancient continental shelf anoxia: an overview. *Modern and Ancient Continental Shelf Anoxia*. Geological Society, London, Special Publication, pp. 1–24.

Welton, J.E. (1984). SEM Petrology Atlas. *The American Association of Petroleum Geologists*

Wigger, P.J., Schmitz, M., Araneda. M., Asch, G., Baldzuhn, S., Giese, P., Heinsohn, W. D., Martinez, E., Ricaidi, E.. Riwer, P. and **Viramonte, J.,** (1994) Variation in the Crustal Structure of the Southern Central Andes Deduced from Seismic Refraction Investigations. *Tectonics of the Southern Central Andes*, pp. 23-48

Winchester, J.A., and **Floyd, P.A**., (1977) Geochemical discrimination of different magma series and their differentiation products using immobile elements. *Chemical Geology*, Vol. 20, pp. 325-343.

Zandt, G., Velasco, A. A. and **Beck, S.L.,** (1994) Composition and thickness of the southern Altiplano crust, Bolivia. *Geology* Vol. 22, pp. 1003-1006.

Zimmermann, U. and **Bahlburg, H.,** (2003) Provenance analysis and tectonic setting of the Ordovician deposits in the southern Puna basin, NW Argentina. *Sedimentology,* Vol. 50 pp. 1079-1104

Zimmermann, U., Niemeyer, H., and **Meffre, S., (2009):** Revealing the continental margin of Gondwana: the Ordovician arc of the Cordón de Lila (Northern Chile). *Springer- Verlag* .

Zimmermann, U., and **Spalletti, L, A., (2009):** Provenance of the Lower Paleozoic Balacrce Formation (Tandilia System, Buenos Aires Province, Argentina): Implication for paleogeographic reconstructions of SW Gondwana. *Sedimentary Geology*, Vol. 219 pp. 7-23.

Zimmermann, U., Poiré D, G., and **Peral, L, G., (2010):** Neoproterozoic to Lower Palaeozoic successions of the Tandilia System in Argentina: implication for the palaeotectonic framework of southwest Gondwana. *Springer- Verlag*

APPENDIX